Published in final edited form as:
Am J Physiol Cell Physiol. 2008 June ; 294(6): . doi:10.1152/ajpcell.00384.2007.

Asymmetric dimethylarginine inhibits HSP90 activity in Pulmonary Arterial Endothelial Cells: Role of Mitochondrial Dysfunction

Neetu Sud[*,1], **Sandra M. Wells**[*,2], **Dean A. Wiseman**[1], **Jason Wilham**[2], and **Stephen M. Black**[1]

[1]Vascular Biology Center, Medical College of Georgia, Augusta GA 30912

[2]Department of Biomedical & Pharmaceutical Sciences, The University of Montana, Missoula, MT30912

Abstract

Increased ADMA levels have been implicated in the pathogenesis of a number of conditions affecting the cardiovascular system. However, the mechanism(s) by which ADMA exerts its effect has not been adequately elucidated. Thus, the purpose of this study was to determine the effect of increased ADMA on nitric oxide (NO) signaling and to begin to elucidate the mechanism by which ADMA acts. Our initial data demonstrated that that ADMA increased NOS uncoupling both in recombinant human endothelial NO synthase (eNOS) and pulmonary arterial endothelial cells (PAEC). Further, we found that this eNOS uncoupling increased 3-nitrotyrosine levels preferentially in the mitochondria of PAEC due to a redistribution of eNOS from the plasma membrane to the mitochondria. This increase in nitration in the mitochondria was found to induce mitochondrial dysfunction as determined by increased mitochondrial derived reactive oxygen species and decreased generation of ATP. Finally, we found that the decrease in ATP resulted in a reduction in the chaperone activity of HSP90 resulting in a decrease in its interaction with eNOS. In conclusion increased levels of ADMA causes mitochondrial dysfunction and a loss of HSP90 chaperone activity secondary to an uncoupling of eNOS. Mitochondrial dysfunction may be an understudied component of the endothelial dysfunction associated with various cardiovascular disease states.

Keywords

peroxynitrite; oxidative stress; mitochondria; protein-protein interactions

INTRODUCTION

There is increasing histologic and physiologic evidence that endothelial injury and the resulting aberration in the balance of its regulatory mechanisms play a major role in the development of vascular dysfunction. Endothelial dysfunction is a hallmark of many diseases of the vasculature, including hypertension (both pulmonary and systemic), atherosclerosis, and diabetes (25, 26). The most important consequence of endothelial dysfunction is the observed decrease in the ability of the endothelium to mediate vasodilation (61). Although the mechanisms involved in the development of endothelial

Please address correspondence and proofs to: Stephen M. Black, Ph.D., Vascular Biology Center: CB-3210B, Medical College of Georgia, 1459 Laney Walker Blvd, Augusta, GA 30912, sblack@mcg.edu.
[*]These authors contributed equally to this work

dysfunction remain incompletely understood, recent studies have suggested that impaired vasodilation in a variety of cardiovascular diseases is linked to the inhibition of NO generation by the amino acid, asymmetric dimethylarginine (ADMA) (4, 6–8, 59). ADMA is an endogenous competitive inhibitor of NOS (4, 6–8, 59). ADMA is constantly produced in the course of normal protein turnover in many tissues, including vascular endothelial cells, and is derived from hydrolysis of methylated proteins (4, 6–8, 59). It appears that both synthesis and degradation of ADMA is regulated in an active manner, and that loss of regulation of either of these pathways may result in elevated levels of ADMA (4, 6–8, 59). Increased ADMA levels have been implicated in the pathogenesis of a variety of conditions affecting the cardiovascular system (4, 6–8, 59) and more recently, also in pulmonary hypertension (2, 37). In addition, several prospective and cross-sectional studies have identified ADMA as a marker of increased cardiovascular risk (4, 6–8, 59).

It has been previously demonstrated that eNOS can interact with a 90kD heat shock protein (HSP90). HSP90 is a member of a molecular chaperone family of proteins which act to modulate protein functions within the cell. HSP90 appears to increase eNOS activity by facilitating the calmodulin induced displacement of caveolin 1 from eNOS (24). This effect can be inhibited with the HSP90 inhibitor geldamycin (21). Several studies show that disruption of HSP90/eNOS interactions attenuates NO production (12, 21, 24, 33, 55) and leads to eNOS uncoupling (46, 47). HSP90 is ATP dependent and the ATPase site of the chaperone is responsible for the autophosphorylation required to enable HSP90 to interact with client proteins (53, 54), suggesting that mitochondrial dysfunction could decrease HSP90 chaperone activity through decreases in cellular ATP levels. Thus, the purpose of this study was to investigate the effect of ADMA on NO and superoxide signaling in pulmonary arterial endothelial cells (PAEC) and to determine if increases in the cellular levels of ADMA leads to the development of mitochondrial dysfunction and if so if this is also associated with a decrease in ATP levels and the disruption of in eNOS/HSP90 interactions.

MATERIALS & METHODS

Purification of recombinant human eNOS

The poly-His-pCWeNOS vector (a gift from Paul Ortiz de Montellano, UCSF) was transformed in to the protease deficient E. coli strain BL21 (DE3) pLysS (Novagen). Cells were grown in Luria broth with 1 % glycerol containing 200μg /ml ampicillin and 40μg/ml chloramphenicol. Cultures were grown at 28°C until an OD_{600} of 0.8 was reached. Approximately one hour before that heme precursor δ-aminolevulinic acid (0.5mM final concentration) was added. Cells were then induced by adding IPTG (0.8mM final concentration), 0.5mM ATP and 3μM riboflavin were also added and the cells were then grown at 22°C for a further 48 hrs in dark. Cells were then harvested by centrifugation (15min at 4,000 × g at 4°C). The cell pellet was resuspended in lysis buffer [40mM N- (2-hydroxyethyl) piperazine-N- (3-Propane sulfonic acid) (EPPS), pH 7.6 containing 1mg/ml lysozyme, 150mM NaCl, 0.5mM L-arginine, 4μM BH_4, 2μM FAD, 10% glycerol and protease inhibitor cocktail (Sigma) were added according to manufacturer's recommendation. The bacterial suspension was incubated with mild shaking at 4°C for 30 minutes to ensure complete cell lysis. Cells were broken by sonication using three 25second pulses followed by three cycles of freezing and thawing. Cell debris was removed by centrifugation at 30,000 × g for 30 min at 4°C .The supernatant was then applied to a Ni-NTA His-Bind Superflow (Novagen) column pre-equilibrated with Buffer A (40mM EPPS, pH 7.6, containing 150mM NaCl, 10% glycerol, and 0.5mM L-arginine. The column was washed with 5 bed volumes of buffer A followed by Buffer B (Buffer A with 25mM Imidazole). The bound protein was then eluted with Buffer C (Buffer A + 200mM Imidazole). The heme containing fractions were pooled and concentrated using

centriprep-100 YM-10 (Millipore). The concentrated protein were dialyzed against three changes of Buffer A containing 4μM BH_4 and 1mM DTT. The protein were further purified by using a 2'5'-ADP-sepharose column equilibrated with 40mM Tris-buffer pH7.6, containing 1mM L-arginine, 3mM DTT, 4μM BH_4, 4μM FAD, 10% glycerol, and 150mM NaCl (Buffer D) and washed with buffer D containing 400mM NaCl to prevent non specific binding. eNOS was then eluted with Buffer E (Buffer D with 5mM 2'AMP). The heme containing fractions were pooled, concentrated and dialyzed at 4°C against buffer D containing 1mM DTT, 4μM BH_4, 4μM FAD, and 10% glycerol and stored at −80°C until used. The DTT, BH_4 and FAD were removed by repeated buffer exchange using centricon prior to use.

Cell culture

Primary cultures of ovine fetal pulmonary artery endothelial cells (PAEC) were isolated as described previously (18). Cells were maintained in DMEM containing phenol red supplemented with 10% fetal calf serum (Hyclone, Logan, UT), antibiotics and antimycotics (MediaTech, Herndon, VA) at 37°C in a humidified atmosphere with 5% CO_2-95% air. Cells were utilized between passages 3 and 10, seeded at 50% confluence, and utilized when fully confluent.

The Y^+ transporter carries both ADMA and L-arginine into the cell. The L arginine levels in our culture medium are 84mg/L (~500μM). Thus, the dose of ADMA used must be able to effectively compete for uptake with L-arginine. For this reason we chose to use 100μM of ADMA. Our initial data indicated that 100μM ADMA rapidly raises intracellular concentrations from ~5μM to ~20μM within 1h (4-fold, Fig. 2A).

Measurement of ADMA

ADMA was analyzed by high-performance liquid chromatography (HPLC) using modifications of a previously described method. Briefly, the crude fraction of cell lysates was isolated using a solid phase extraction column and subsequently, ADMA was separated using precolumn derivitization with σ-phthaldialdehyde (OPA) reagent (4.5 mg/mL in borate buffer, pH 8.5, containing 3.3 μl/mL β-mercaptoethanol) prior to injection. HPLC was performed using an Amersham Biosciences AKTA purifier system (GE Healthcare, Piscataway, NJ) with a Nucleosil Phenyl reverse phase column (4.6×250 mm; Supelco, Bellefonte, PA), equipped with a Jasco FP-2020 fluorescence detector (Jasco Corporation, Tokyo, Japan). ADMA levels were quantified by fluorescence detection at 450 nm (emission) and 340 nm (excitation). Mobile phase A was composed of 95% potassium phosphate (50 mM, pH 6.6), 5% methanol and mobile phase B was composed of 100% methanol. ADMA was separated using a pregradient wash of 25% mobile phase B (flow rate 0.8 mL/min), followed by a linear increase in mobile phase B concentration from 20% to 25% over 7 minutes followed by a constant flow at 25% for 10 minutes and another linear increase from 25% to 27% mobile phase B over 5 minutes followed by constant flow at 27% mobile phase B for another 7 minutes. Retention time for ADMA was approximately 28 minutes. ADMA concentrations were calculated using standards and an internal homoarginine standard. The detection limit of the assay was 0.1 μmol/L.

HSP90 immunoprecipitation and Western blotting

PAEC were exposed or not to ADMA (100μM) then solubilized with a lysis buffer containing 1% Triton X-100, 20mM Tris pH 7.4, 100mM NaCl, 1 mM EDTA, 1% sodium deoxycholate, 0.1% SDS and protease inhibitor cocktail (Pierce). Insoluble proteins were precipitated by centrifugation at 13,000 rpm for 10 min at 4°C, and the supernatants were then incubated overnight with the anti-HSP90 antibody (2 μg) at 4°C followed by incubation in Protein G plus protein A agarose (Calbiochem) for 2 hours. The immune complexes were

precipitated by centrifugation, washed three times with lysis buffer, boiled in SDS sample buffer, and subjected to SDS-PAGE on 4–12% polyacrylamide gels and transferred to a nitrocellulose membrane (Biorad). The membranes were blocked with 5% nonfat dry milk in Tris-buffered saline containing 0.1% Tween (TBST). The primary antibody, eNOS (1:500, BD Transduction Laboratories), was then added and incubated for 1h at room-temperature. The membrane was then washed three times with TBST (10min) then incubated with a secondary antibody coupled to horseradish peroxidase. The membrane was then washed three times with TBST as described above. Reactive bands were visualized using the SuperSignal® West Femto Maximum Sensitivity Substrate Kit (Pierce, Rockford, IL, USA) and Kodak 440CF image station (Kodak, New Haven, CT, USA). The intensity of the reactive bands was quantified using the Kodak 1D software. The efficiency of each immunoprecipitation was normalized by reprobing the membrane with the immunoprecipitating antibody (HSP90).

DHE fluorescence analysis

PAEC were seeded onto 96-well plates (Costar) and allowed to adhere for at least 18 hours. Cells were then washed in PBS and incubated in serum-free DMEM in the presence or absence of ADMA (100μM, 1h). Dihydroethidium (DHE; 5μM; Molecular Probes) was added to the media 15 minutes before the end of the experiment. Oxidation of DHE was observed after excitation at 518nm and emission at 605nm as described below.

Plasma membrane Isolation

Plasma membrane was isolated from ADMA treated and untreated cells using Pierce Mem-PER Eukaryotic Membrane Protein Extraction Reagent Kit according to manufacturer's protocol. Briefly, 5×10^6 cells were pelleted by centrifugation then lyzed. The supernatant obtained by centrifugation at 10,000 ×g for 3min. was incubated at room temperature for 20min. The tubes were centrifuged at 10,000 × g for 2min and the hydrophobic phase (bottom layer) was carefully separated from hydrophilic phase (top layer). The hydrophobic phase contains the plasma membrane fraction.

Mitochondria Isolation

Following ADMA treatment for 1 hr, the mitochondria were isolated using Pierce Mitochondria isolation kit using manufacturer's protocol. Briefly, 2×10^7 were pelleted by centrifugation at 850 × g for 2 min. and Mitochondria Isolation Reagent A was added to the pellet. Cells were vortexed for 5 seconds then incubated on ice for 2 min. Mitochondria Isolation Reagent B was added, followed by vortexing for 5 seconds. Tubes were incubated on ice for 5min, vortexing being done every 1 min. Mitochondria Isolation Reagent C was added and the tubes inverted several times to mix. The supernatant obtained by centrifugation at 700 × g for 10min at 4°C was transferred to a new tube and centrifuged at 3,000×g for 15min. Mitochondria Isolation Reagent C was added to the pellet and centrifuged at 12,000 × g for 5min. The pellet contains the mitochondrial fraction. To determine the effect of eNOS inhibition on ADMA induced eNOS translocation, cells were treated for 30min with ethylisothiourea (ETU, 100μM) prior to addition of ADMA. To detect how L-arginine effects ADMA mediated eNOS translocation, L-arginine (500μM) was added along with ADMA. To determine the effect of SOD on ADMA stimulated eNOS translocation, cells were pretreated with 100U/ml PEG-SOD (30 min) prior to ADMA addition.

Detection of mitochondrial superoxide levels

Mitochondrial superoxide production was measured using MitoSOX™ Red mitochondrial superoxide indicator (Molecular Probes), a fluorogenic dye for selective detection of

superoxide in the mitochondria of live cells. MitoSOX Red reagent is live-cell permeant, and is rapidly and selectively targeted to the mitochondria. Once in the mitochondria, MitoSOX Red reagent is oxidized by superoxide and exhibits bright red fluorescence upon binding to nucleic acids. Briefly, PAEC were treated with ADMA (100μM, 30 min.), cells were washed with fresh media, and then incubated in media containing MitoSOX Red (2 μM) and ADMA (100μM), for a further 30 min. at 37°C in dark conditions. Cells were washed with fresh serum-free media and imaged using fluorescence microscopy as described below using an excitation of 510 nm and an emission at 580 nm.

Fluorescence Microscopy

A PC-based imaging system consisting of the following components: an Olympus IX51 microscope equipped with a CCD camera (Hamamatsu Photonics, Hamamatsu City, Japan) was used for acquisition of fluorescent images. Fluorescent-stained cells were observed with the appropriate excitation and emission, and the average fluorescent intensities (to correct for differences in cell number) were quantified using ImagePro Plus v.5.0 imaging software (Media Cybernetics, Silver Spring, MD).

EPR spectroscopy and spin trapping

To detect superoxide generation in intact cells, EPR measurements were performed as described previously (65). Following overnight serum starvation of the cells, 20 μl of spin-trap stock solution consisting of 1-hydroxy-3-methoxycarbonyl-2,2,5,5-tetramethylpyrrolidine·HCl (CMH, Alexis Biochemicals, San Diego, CA) 20 μM in DPBS +25 μM desferrioxamine (Calbiochem, La Jolla, CA) and 5 μM diethyldithiocarbamate (Alexis Biochemicals, Lausen, Switzerland) + 2 μl DMSO were added to each well prior to shear stimulation. Adherent cells were trypsinized and pelleted at 500 *g* after a 45 min incubation at 37°C post shear to allow entrapment of superoxide by the spin trap. Cell pellet was washed and suspended in a final volume of 35 μl DPBS (containing desferrioxamine and diethyldithiocarbamate), loaded into a 50-μl capillary tube and analyzed with a MiniScope MS200 EPR Magnettech, Berlin, Germany) at a microwave power of 40 mW, modulation amplitude of 3,000 mG, and modulation frequency of 100 kHz. EPR spectra were analyzed measured for amplitude using ANALYSIS software (version 2.02; Magnettech) and experimental groups were compared using statistical analysis described below. In the experiments examining the role of ADMA in modulating superoxide production, the cells were preincubated with the ADMA (100μM) for 30 min. before the addition of the CMH. To determine the effect of eNOS inhibition on ADMA induced superoxide production, cells were treated for 30min with ethylisothiourea (ETU, 100μM) prior to addition of ADMA. To detect how L-arginine effects ADMA mediated superoxide generation, Larginine (500μM) was added along with ADMA. To determine the effect of SOD on ADMA stimulated superoxide generation, cells were pretreated with 100U/ml PEG-SOD (30 min) prior to ADMA addition. EPR measurements were performed as described above.

Effect of ADMA on NO_x and superoxide generation by eNOS in vitro

The *in vitro* reaction was conducted in 50 μl of buffer containing 50 mM HEPES (pH 7.4), 1 mM NADPH, 100 μM L-arginine, 1 mM Ca^{2+}, 10 μg/ml calmodulin, 4 μM tetrahydrobiopterin, 1μg eNOS$^{\cdot\cdot}$ Endothelial NOS dependent superoxide generation *in vitro* was performed in 50 μl of reaction mix containing 50 mM HEPES (pH 7.4), 1 mM NADPH, 1 mM Ca^{2+}, 10 μg/ml calmodulin, 4 μM tetrahydrobiopterin, 1μg eNOS.and CMH hydrochloride. In the experiments determining the effect of ADMA, eNOS and HSP90 were incubated for 15 min before measurements were made. The effect of ADMA on superoxide generation as then determined as described above. The effect of ADMA on NO generation was determined using an NO-sensitive electrode with a 2-mm diameter tip (ISO-NOP

sensor, WPI) connected to an NO meter (ISO-NO Mark II, WPI) as described previously (65).

Effect of ADMA on superoxide dismutase activity

Endothelial cells from fetal lamb were treated with ADMA for 1 hour and SOD activity in treated and untreated cells was measured using Cayman Chemical Superoxide Dismutase Assay Kit according to manufacturer's instructions. The method utilizes a tetrazolium salt to quantify superoxide radicals generated by xanthine oxidase and hypoxanthine. Briefly, cells were lysed in 20mM HEPES buffer pH 7.2 containing 1mM EGTA, 210mM mannitol and 70mM sucrose, centrifuged at 1500×g for 5 minutes at 4°C and the and the supernatant was collected for SOD assay. The samples and standards were added in duplicate to a sample plate provided with the kit. Reactions were initiated by adding xanthine oxidase to all wells, and the samples were incubated on a shaker at room temperature for 20 min. The absorbance of each standard and sample was read at 450 nm by the use of an absorbance microplate reader. SOD activity was calculated from the linear regression of the standard curve by substituting the linearized rate for each sample. One unit was defined as the amount of enzyme needed to exhibit 50% dismutation of the $O_2^{-}\cdot$ radical.

Dot-Blot Analysis for 3-Nitrotyrosine

Mitochondrial fractions (50μg) prepared from PAEC exposed to ADMA (100μM, 0–8h) were blotted onto nitrocellulose membranes using a Bio Dot apparatus (Bio-Rad, Hercules, CA). The membrane was rinsed in 20 ml TBST and blocked with 20 ml 5% nonfat milk in TBST for 1hour, followed by an incubation with a 3-Nitrotyrosine antibody (1:1000, Calbiochem, San Diego, CA) at 4° C overnight. After three washes with TBST, the membrane was incubated with goat antimouse IgG HRP conjugated secondary antibody (1:2000, Pierce, Rockford, IL) for 1h at room temperature. After washing, the dots were visualized with chemiluminescence using a Kodak Digital Science ™ Image Station (NEN) and analyzed using the KED-1 software. All captured and analyzed images were determined to be in the dynamic range of the system. The same membrane was then probed with β-actin to normalize for loading.

Detection of NO_x in pulmonary arterial endothelial cells

NO generated by PAECs was measured using an NO-sensitive electrode with a 2-mm diameter tip (ISO-NOP sensor, WPI) connected to an NO meter (ISO-NO Mark II, WPI) as described previously (33).

Cellular ATP Levels

Assay for ATP was done using the firefly luciferin-luciferase method uing a commercially available kit (Invitrogen). ATP is consumed and light is emitted when firefly luciferase catalyzes the oxidation of luciferin. The amount of light emitted during the reaction is proportional to the availability of ATP. Luminescence was measured using a Fluoroscan Ascent FL luminometer (Thermo Electron, Corp.).

Statistical Analysis

Statistical calculations were performed using the GraphPad Prism V. 4.01 software. The mean ± SEM was calculated for all samples and significance determined by either by the unpaired t-test or ANOVA. A value of $P < 0.05$ was considered significant.

RESULTS

Effect of ADMA on superoxide and NO production by eNOS in vitro

To investigate the effect of ADMA on eNOS uncoupling we initially utilized recombinant human eNOS. Our data indicate that superoxide production from eNOS was significantly enhanced (Fig. 1 A, P<0.05 vs. no ADMA) in the presence of ADMA while the NO produced was significantly diminished (Fig. 1 B, P<0.05 vs. no ADMA).

Effect of ADMA on superoxide generation in pulmonary arterial endothelial cells

To begin to determine the significance of increased ADMA levels on superoxide generation in PAEC we initially determined the effect of adding exogenous ADMA to intracellular ADMA concentrations. Our data indicate that the addition of ADMA (100μM, 1h) to PAEC resulted in a significant (4.3-fold) increase in intracellular ADMA levels (Fig. 2 A, P <0.05 vs Control). We next examined the effect of ADMA on NOS-dependent superoxide production utilizing the oxidation to dihydroethidium to ethidium. Superoxide generation was found to be significantly increased in ADMA exposed PAEC (Fig. 2 B, *P*<0.05 vs. control). This ADMA-mediated increase in superoxide formation was blocked in the presence of the NOS-inhibitor, ETU indicating that ADMA also induces eNOS uncoupling in PAEC (Fig. 2 B, P<0.05 vs. ADMA alone). We subsequently confirmed this ADMA-mediated increase in superoxide generation using EPR analysis (Fig. 2 C). Further, this increase in NOS-derived superoxide was associated with a decrease in NO generation (Fig. 2 D).

To confirm that the ADMA-mediated increase in superoxide was due to uncoupling of eNOS, cells were pretreated with the non-specific NOS inhibitor, ETU. ETU caused a significant decrease in ADMA treated cells (Fig. 2 C). Further, we found that the addition of excess L-arginine (which competes with ADMA for the Y^+-transporter), or the superoxide scavenger, PEG-SOD both significantly reduced the ADMA-mediated increase in superoxide (Fig. 2 C). In addition, we found that ADMA did not alter SOD activity in the cell indicating that the increase in superoxide was not due to a loss of SOD activity (Fig. 3).

ADMA increases 3-nitrotyrosine levels in pulmonary arterial endothelial cells

As ADMA appeared to be causing uncoupling of eNOS we next determined whether this induced 3-NT levels in PAEC (as a surrogate marker for peroxynitrite generation). Utilizing dot-blot analysis we found that 3-NT levels were significantly increased in whole cell extracts of PAEC exposed to ADMA (Fig. 4 A, P<0.05 vs. Control). Similar increases in 3-NT levels were also observed in isolated mitochondria from ADMA-exposed PAEC although the duration of the increase in 3-NT levels was longer (Fig. 4 B, P<0.05 vs. Control).

ADMA stimulates eNOS redistribution to the mitochondrion

To further investigate the mechanism for the potentiated effect of ADMA on protein nitration within the mitochondria we isolated plasma membrane and mitochondria from control and ADMA treated PAEC and subjected them to Western blot analysis. Our data indicate that ADMA stimulated a redistribution of eNOS from the plasma membrane (Fig. 5 A & B, P<0.05 vs. Control) to the mitochondria (Fig. 5 C & D, P<0.05 vs. Control).

The ADMA-mediated mitochondrial redistribution is peroxynitrite dependent

To further investigate the mechanism for the redistribution of eNOS from the plasma membrane to the mitochondria we evaluated the role of the peroxynitrite produced by the ADMA-mediated uncoupling of eNOS. Our data indicated that the NOS inhibitor, ETU

caused a significant decrease in the ADMA-mediated eNOS mitochondrial translocation cells (Fig. 6 A & B). Further, we found that the addition of excess L-arginine (which competes with ADMA for the Y^+-transporter), or the superoxide scavenger, PEG-SOD also both significantly reduced the ADMA-mediated eNOS mitochondrial translocation (Fig. 6 A & B). Further, the peroxynitrite generator, SIN-1 alone is able to stimulate eNOS translocation to the mitochondria (Fig. 6 C & D) while the peroxynitrite scavenger, MnTymPyp reduces ADMA-mediated eNOS mitochondrial translocation (Fig. 6 C & D). Together, these data suggest a role for peroxynitrite in regulating the mitochondrial translocation of eNOS.

ADMA induces mitochondrial oxidative stress and increases UCP-2 expression in pulmonary arterial endothelial cells

To determine if the increase in nitrated proteins in the mitochondria of ADMA-exposed cells was altering mitochondrial function we utilized MitoSOX that we have previously shown to be a good marker of oxidative stress in the mitochondria (64, 65). We found that oxidative stress within the mitochondria was significantly increased in ADMA exposed cells (Fig. 7, $P<0.05$ vs. Control). Further, our data indicate that ADMA-exposed cells have a significantly increased expression of the mitochondrial uncoupling protein, UCP-2 (Fig. 8, $P<0.05$ vs. Control).

ADMA decreases ATP levels in pulmonary arterial endothelial cells

To determine if the ADMA-induced increase in mitochondrial oxidative stress was altering mitochondrial function we next investigated the effect of ADMA on cellular ATP levels. Our data indicate that ADMA caused a significant reduction in cellular ATP levels that was maintained for at least 8h (Fig. 9, $P<0.05$ vs. control).

ADMA disrupts the interaction of HSP90 with eNOS

As mentioned previously the chaperone activity of HSP90 is ATP dependent. Thus, we examined the effect of the ADMA-mediated decrease in cellular ATP levels on HSP90 activity by examining eNOS/HSP90 interactions. To accomplish this we utilized immunoprecipitation. Western blotting for eNOS on the immunoprecipitated HSP90 complex revealed that ADMA exposure led to significant decrease in the association of HSP90 with eNOS (Fig. 10 A, $P<0.05$ vs. Control) and Ser1177-phospho-eNOS (Fig. 10 B, $P<0.05$ vs. Control) in PAEC.

DISCUSSION

The important findings of this study are as follows: 1) ADMA stimulates the redistribution of eNOS from the plasma membrane to the mitochondrion; 2) ADMA uncouples eNOS both *in vitro* and in PAEC; 3) The increased generation of peroxynitrite lis required for eNOS redistribution to the mitochondrion; 4) The uncoupled eNOS localized to the mitochondrion results in an increase in nitrated proteins in the mitochondria; 5) These nitration events leads to mitochondrial dysfunction and reduced cellular ATP levels; 6) The reduction in ATP leads to a decrease in the chaperone activity of HSP90; that 7) decreases the interaction of HSP90 with eNOS further reducing NO signaling.

A number of studies suggest that impaired vasodilation in a variety of cardiovascular diseases is linked to the inhibition of NO generation by the amino acid, asymmetric dimethylarginine (ADMA) (4, 6–8, 59). ADMA is an endogenous competitive inhibitor of NOS (4, 6–8, 59). ADMA is continuously produced in the course of normal protein turnover in tissues, including vascular endothelial cells, and is derived from hydrolysis of methylated proteins (4, 6–8, 59). Elevated plasma levels of ADMA have been reported in heart failure

(19), atherosclerosis (38), diabetes mellitus(34), and hypertension(23). Further, Gorenflo et al found ADMA plasma levels in patients with severe pulmonary hypertension were significantly increased (median, 0.55 μM/l; range, 0.25–0.79 μM/l) compared to control patients (median, 0.21 μM/l; range, 0.08–0.27 μM/l) (23). This increase may account for the endothelial vasodilator dysfunction observed in this condition. Also, Boger and colleagues previously demonstrated that cultured human endothelial cells produce superoxide (as determined by increased oxidation of DHE) in the presence of ADMA (9). This led to the hypothesis that ADMA may interrupt the NO-producing activity of NOS and "uncouple" the enzyme, which results in a "switch" of the enzymatic activity from NO to superoxide (9). The data we present here demonstrate that ADMA can uncouple eNOS both *in vitro*, using recombinant purified human eNOS, and in cultured PAEC. The direct uncoupling effect of ADMA on eNOS is interesting as a recent study found that ADMA does not uncouple purified neuronal NOS (nNOS) (13). These differing effects of ADMA on NOS isoforms with regard to NOS uncoupling suggest that ADMA may exert effects that are isoform dependent and future studies to examine the effect of ADMA on inducible NOS coupling will also be required. Further, our data indicate that the increased eNOS uncoupling in ADMA exposed cells results in an increase in nitrated protein both in whole cell extracts and in isolated mitochondria. However, the effect on the mitochondria appears to be more sustained (6h vs. 1h). This is likely due to the fact that ADMA stimulates the redistribution of eNOS from the plasma membrane to the mitochondrion. Endothelial NOS redistribution to the outer mitochondrial membrane has been shown previously in both human umbilical vein endothelial cells and in human embryonic kidney cells transiently transfected with an eNOS expression construct (20). The key sequence required for mitochondrial localization has been localized to residues 628–632 (20). This sequence is located within the 45 amino acid autoinhibitory domain of eNOS that is an insertion in the FMN-containing domain and is thought to have an important role in regulating eNOS activity (51). Further studies will be required to determine if ADMA acts on these same residues to stimulate the redistribution of eNOS. Alternatively, it is also possible that the mitochondrion lacks the ability to remove nitrated proteins effectively including nitrated eNOS. Furthermore, our data indicate that the elevations in cellular and mitochondrial 3NT decrease with time and that the cells are responding to the ADMA-challenge. The mechanism by which occurs is not clear from our studies. However, one possible explanation is that as ADMA is actively degraded by DDAH, over-time intracellular ADMA concentrations will tend to diminish as we added only one bolus dose of ADMA. Thus, eNOS uncoupling will also tend to diminish which would explain the recovery of the cells over time. Similarly, this could explain the apparent recovery of ATP levels in the cell. In addition, the mechanism by which ATP levels diminish is unclear. However, our recent in vivo studies in a lamb model of pulmonary hypertension secondary to increased pulmonary blood flow have shown that Indeed our peroxynitrite mediated nitration of the mitochondrial protein, carnitine acetyl trasnferase (CrAT) may be important for the loss of mitochondrial function. Thus, it is possible that the nitration-mediated by ADMA leads to an inhibition of CrAT and subsequent decreases in ATP levels. Further studies will be required to test these possibilities.

With increasing knowledge of the role of ADMA in the pathogenesis of cardiovascular disease, ADMA is likely to become a goal for pharmacotherapeutic interventions (5). Several studies support the view that the ratio between L-arginine and ADMA is a key component in the regulation of endothelial NOS activity and elevated ADMA levels have been shown to antagonize endothelium-dependent vasodilation in humans (4, 6–8, 59) and the administration of L-arginine has been shown to improve endothelium-dependent vascular functions in subjects with high ADMA levels (10). ADMA can be metabolized via hydrolytic degradation to citrulline and dimethylamine by the enzyme dimethylarginine dimethylaminohydrolase (DDAH) (6). There are two currently identified isoforms of DDAH: 1 & 2 (11, 38). The endothelial cell predominant isoform is believed to be DDAH2

(31, 59) and the inhibition of DDAH activity results in vasoconstriction of vascular segments that can be reversed by L-arginine (35). The regulation of DDAH is not fully understood. However, in endothelial cells, oxidative stress induced by oxLDL or TNF-α has been shown to decrease DDAH activity (30) while Lin and colleagues have shown that elevated glucose raises endothelial ADMA levels by inhibiting DDAH activity (34). Conversely, in an interesting study from Tran and co-workers all-trans-Retinoic acid (atRA) increased nitrite production by sEnd.1 cells without increasing eNOS expression. Rather, atRA was shown to increase DDAH II gene expression and promoter activity with a subsequent reduction in ADMA levels. However, further studies will be required to determine if altering the ADMA: L-arginine ratio with arginine supplementation or stimulating DDAH activity will reduce the mitochondrial dysfunction that we have found with elevated levels of ADMA.

Disruption of mitochondrial function is acknowledged as a critical event in a number of pathologic conditions including hypoxia-ischemic injuries (3), stroke (56), and diabetes (17, 39, 41, 44). There is also evidence for decreased mitochondrial function in aging related neurodegenerative disorders (18, 22). In addition, a study in poultry has shown that lung mitochondrial dysfunction is present in broilers with pulmonary hypertension syndrome and this was associated with oxidative stress as high dietary vitamin E attenuated the effect (29). Mitochondria are the source of superoxide anion radicals and hydrogen peroxide (H_2O_2) under physiologic and pathologic conditions. The increased production of ROS from the mitochondria can be deleterious to the cell due to their ability to induce lipid peroxidation, protein oxidation, and DNA damage (49, 60). Indeed we, and others, have shown that reactive nitrogen species such as nitric oxide and peroxynitrite can lead to increased mitochondrial ROS production (27, 43, 65). The mechanisms for these effects appear to involve the inhibition of mitochondrial complexes-I and -III (27, 43) as well as the disruption of zinc homeostasis (65). The data we present here indicate that mitochondrial dysfunction can also decrease HSP90 chaperone activity secondary to a loss of normal ATP generation. This reduction in HSP90 activity could have significant effects on cell function. With respect to endothelial biology and NO signaling HSP90 is known to interact with a number of proteins required for efficient NO biosynthesis including eNOS (24), soluble guanylate cyclase (42, 62), and possibly GTP cyclohydrolase (58). A loss of normal activity for any of these proteins would have a significant deleterious effect on NO signaling. However the effects of a decrease in HSP90 activity would extend far beyond NO signaling. HSP90 is an essential chaperone for the proper folding of a large number of proteins. The importance of HSP90 function is demonstrated by the fact that in eukaryotes, the activity of HSP90 is essential for cell viability. The function of HSP90 is highly complex with recent studies only now beginning to identify signaling networks that are dependent of a functional HSP90. The complexity of these interactions have been demonstrated using the lower eukaryote, Saccharomyces cerevisiae where HSP90 has been shown to interact directly or indirectly with more than 10% of all proteins in the cell. Thus, any decreases in the activity of the HSP90 system could have dramatic effects on cell survival.

An oversupply of electrons in the mitochondrial transfer chain can also result in mitochondrial membrane hyperpolarization and the formation of ROS (16, 32, 50, 63). These free radicals damage proteins and lipids and lead to dysfunction of mitochondria, the central mediators of programmed cell death (16, 32, 50, 63). Damaged mitochondria release proapoptotic factors that activate the cysteine protease family of caspases, which in turn propagate a death cascade (16, 32, 50, 63). Cellular energy and mitochondrial membrane function are regulated in part by the uncoupling proteins (UCPs) (14, 48). UCPs are mitochondria carrier proteins that dissipate the proton gradient of the inner mitochondria membrane. This uncoupling reaction can bypass the production of ATP by oxidative phosphorylation (14, 48). Increased expression of UCP isoforms is believed to be a marker

of mitochondrial dysfunction (1, 28, 36, 40, 57). The different members of the UCP family have distinct tissue distributions (15, 45, 52). Tissue localization as well as regulation confers different roles for the family members. For example, UCP1 is strictly restricted to brown adipose tissue, and its principal function is believed to be the generation of body heat (15, 45, 52). UCP3 tissue distribution is predominantly limited to skeletal muscle, whereas UCP2 expression is widespread (15, 45, 52). However, it is still unclear the exact role of UCP proteins in mitochondrial dysfunction and how their expression and activation are regulated have not been adequately resolved. Our data here link increased nitrosative stress in the mitochondria with increased UCP-2 expression suggesting that mitochondrial dysfunction may be a signal for the cell to increase UCP-2 expression. Recent investigations have demonstrated that UCP can also prevent mitochondrial damage during stroke (57) suggesting that increased expression of UCP may be an adaptive response for the cell to try and protect the mitochondria after an insult. However, further studies will be required to determine if increases in UCP-2 expression are protective for the mitochondria in ADMA challenged PAEC.

In conclusion, our data suggest that increased levels of ADMA can induce mitochondrial dysfunction in PAEC with a resulting decrease in cellular ATP levels and HSP90 chaperone activity. Further, our data emphasize that mitochondrial dysfunction may be an understudied aspect of cardiovascular disorders, and that therapies aimed at maintaining mitochondrial function may have beneficial effects on endothelial function in these pathologic states.

Acknowledgments

This research was supported in part by grants HL60190 (SMB), HL67841 (SMB), HL072123 (SMB), and HL070061 (SMB) all from the National Institutes of Health, 0550133Z from the American Heart Association, Pacific Mountain Affiliates (SMB), and by a grant from the Fondation Leducq (SMB). The authors would also like to thank Dr. Jeff Fineman for critical reading of this manuscript.

REFERENCES

1. Andrews ZB, Diano S, Horvath TL. Mitochondrial uncoupling proteins in the CNS: in support of function and survival. Nature reviews. 2005; 6:829–840.
2. Arrigoni FI, Vallance P, Haworth SG, Leiper JM. Metabolism of asymmetric dimethylarginines is regulated in the lung developmentally and with pulmonary hypertension induced by hypobaric hypoxia. Circulation. 2003; 107:1195–1201. [PubMed: 12615801]
3. Blomgren K, Zhu C, Hallin U, Hagberg H. Mitochondria and ischemic reperfusion damage in the adult and in the developing brain. Biochem Biophys Res Commun. 2003; 304:551–559. [PubMed: 12729590]
4. Boger RH. Association of asymmetric dimethylarginine and endothelial dysfunction. Clin Chem Lab Med. 2003; 41:1467–1472. [PubMed: 14656027]
5. Boger RH. Asymmetric dimethylarginine (ADMA) modulates endothelial function--therapeutic implications. Vasc Med. 2003; 8:149–151. [PubMed: 14989553]
6. Boger RH. Asymmetric dimethylarginine, an endogenous inhibitor of nitric oxide synthase, explains the "L-arginine paradox" and acts as a novel cardiovascular risk factor. J Nutr. 2004; 134:2842S–2847S. discussion 2853S. [PubMed: 15465797]
7. Boger RH. The emerging role of asymmetric dimethylarginine as a novel cardiovascular risk factor. Cardiovasc Res. 2003; 59:824–833. [PubMed: 14553822]
8. Boger RH, Bode-Boger SM. Asymmetric dimethylarginine, derangements of the endothelial nitric oxide synthase pathway, and cardiovascular diseases. Semin Thromb Hemost. 2000; 26:539–545. [PubMed: 11129410]
9. Boger RH, Bode-Boger SM, Tsao PS, Lin PS, Chan JR, Cooke JP. An endogenous inhibitor of nitric oxide synthase regulates endothelial adhesiveness for monocytes. J Am Coll Cardiol. 2000; 36:2287–2295. [PubMed: 11127475]

10. Boger RH, Ron ES. L-Arginine improves vascular function by overcoming deleterious effects of ADMA, a novel cardiovascular risk factor. Altern Med Rev. 2005; 10:14–23. [PubMed: 15771559]
11. Boger RH, Vallance P, Cooke JP. Asymmetric dimethylarginine (ADMA): a key regulator of nitric oxide synthase. Atheroscler Suppl. 2003; 4:1–3. [PubMed: 14664896]
12. Bucci M, Roviezzo F, Cicala C, Sessa WC, Cirino G. Geldanamycin, an inhibitor of heat shock protein 90 (Hsp90) mediated signal transduction has anti-inflammatory effects and interacts with glucocorticoid receptor in vivo. Br J Pharmacol. 2000; 131:13–16. [PubMed: 10960063]
13. Cardounel AJ, Xia Y, Zweier JL. Endogenous methylarginines modulate superoxide as well as nitric oxide generation from neuronal nitric oxide synthase: Differences in the effects of monomethyl and dimethyl arginines in the presence and absence of tetrahydrobiopterin. J Biol Chem. 2004
14. Chan CB, Saleh MC, Koshkin V, Wheeler MB. Uncoupling protein 2 and islet function. Diabetes. 2004; 53(Suppl 1):S136, S142. [PubMed: 14749279]
15. Dridi S, Onagbesan O, Swennen Q, Buyse J, Decuypere E, Taouis M. Gene expression, tissue distribution and potential physiological role of uncoupling protein in avian species. Comp Biochem Physiol A Mol Integr Physiol. 2004; 139:273–283. [PubMed: 15556382]
16. Droge W. Free radicals in the physiological control of cell function. Physiol Rev. 2002; 82:47–95. [PubMed: 11773609]
17. Duchen MR. Roles of mitochondria in health and disease. Diabetes. 2004; 53(Suppl 1):S96, S102. [PubMed: 14749273]
18. Emerit J, Edeas M, Bricaire F. Neurodegenerative diseases and oxidative stress. Biomed Pharmacother. 2004; 58:39–46. [PubMed: 14739060]
19. Feng Q, Lu X, Fortin AJ, Pettersson A, Hedner T, Kline RL, Arnold JM. Elevation of an endogenous inhibitor of nitric oxide synthesis in experimental congestive heart failure. Cardiovasc Res. 1998; 37:667–675. [PubMed: 9659450]
20. Gao S, Chen J, Brodsky SV, Huang H, Adler S, Lee JH, Dhadwal N, Cohen-Gould L, Gross SS, Goligorsky MS. Docking of endothelial nitric oxide synthase (eNOS) to the mitochondrial outer membrane: a pentabasic amino acid sequence in the autoinhibitory domain of eNOS targets a proteinase K-cleavable peptide on the cytoplasmic face of mitochondria. J Biol Chem. 2004; 279:15968–15974. [PubMed: 14761967]
21. Garcia-Cardena G, Fan R, Shah V, Sorrentino R, Cirino G, Papapetropoulos A, Sessa WC. Dynamic activation of endothelial nitric oxide synthase by Hsp90. Nature. 1998; 392:821–824. [PubMed: 9580552]
22. Genova ML, Pich MM, Bernacchia A, Bianchi C, Biondi A, Bovina C, Falasca AI, Formiggini G, Castelli GP, Lenaz G. The mitochondrial production of reactive oxygen species in relation to aging and pathology. Ann N Y Acad Sci. 2004; 1011:86–100. [PubMed: 15126287]
23. Gorenflo M, Zheng C, Werle E, Fiehn W, Ulmer HE. Plasma levels of asymmetrical dimethyl-L-arginine in patients with congenital heart disease and pulmonary hypertension. J Cardiovasc Pharmacol. 2001; 37:489–492. [PubMed: 11300662]
24. Gratton JP, Fontana J, O'Connor DS, Garcia-Cardena G, McCabe TJ, Sessa WC. Reconstitution of an endothelial nitric-oxide synthase (eNOS), hsp90, and caveolin-1 complex in vitro. Evidence that hsp90 facilitates calmodulin stimulated displacement of eNOS from caveolin-1. J Biol Chem. 2000; 275:22268–22272. [PubMed: 10781589]
25. Griendling KK, Sorescu D, Lassegue B, Ushio-Fukai M. Modulation of protein kinase activity and gene expression by reactive oxygen species and their role in vascular physiology and pathophysiology. Arterioscler Thromb Vasc Biol. 2000; 20:2175–2183.
26. Griendling KK, Sorescu D, Ushio-Fukai M. NAD(P)H oxidase: role in cardiovascular biology and disease. Circ Res. 2000; 86:494–501. [PubMed: 10720409]
27. Han Z, Chen YR, Jones CI 3rd, Meenakshisundaram G, Zweier JL, Alevriadou BR. Shear-induced reactive nitrogen species inhibit mitochondrial respiratory complex activities in cultured vascular endothelial cells. Am J Physiol Cell Physiol. 2007; 292:C1103–C1112. [PubMed: 17020931]

28. Hoffstedt J, Folkesson R, Wahrenberg H, Wennlund A, van Harmelen V, Arner P. A marked upregulation of uncoupling protein 2 gene expression in adipose tissue of hyperthyroid subjects. Horm Metab Res. 2000; 32:475–479. [PubMed: 11246812]
29. Iqbal M, Cawthon D, Wideman RF Jr, Bottje WG. Lung mitochondrial dysfunction in pulmonary hypertension syndrome. II. Oxidative stress and inability to improve function with repeated additions of adenosine diphosphate. Poult Sci. 2001; 80:656–665. [PubMed: 11372718]
30. Ito A, Tsao PS, Adimoolam S, Kimoto M, Ogawa T, Cooke JP. Novel mechanism for endothelial dysfunction: dysregulation of dimethylarginine dimethylaminohydrolase. Circulation. 1999; 99:3092–3095. [PubMed: 10377069]
31. Jones LC, Tran CT, Leiper JM, Hingorani AD, Vallance P. Common genetic variation in a basal promoter element alters DDAH2 expression in endothelial cells. Biochem Biophys Res Commun. 2003; 310:836–843. [PubMed: 14550280]
32. Kannan K, Jain SK. Oxidative stress and apoptosis. Pathophysiology. 2000; 7:153–163. [PubMed: 10996508]
33. Khurana VG, Feterik K, Springett MJ, Eguchi D, Shah V, Katusic ZS. Functional interdependence and colocalization of endothelial nitric oxide synthase and heat shock protein 90 in cerebral arteries. Journal of Cerebral Blood Flow & Metabolism. 2000; 20:1563–1570. [PubMed: 11083231]
34. Lin KY, Ito A, Asagami T, Tsao PS, Adimoolam S, Kimoto M, Tsuji H, Reaven GM, Cooke JP. Impaired nitric oxide synthase pathway in diabetes mellitus: role of asymmetric dimethylarginine and dimethylarginine dimethylaminohydrolase. Circulation. 2002; 106:987–992. [PubMed: 12186805]
35. MacAllister RJ, Parry H, Kimoto M, Ogawa T, Russell RJ, Hodson H, Whitley GS, Vallance P. Regulation of nitric oxide synthesis by dimethylarginine dimethylaminohydrolase. Br J Pharmacol. 1996; 119:1533–1540. [PubMed: 8982498]
36. Mattson MP, Liu D. Mitochondrial potassium channels and uncoupling proteins in synaptic plasticity and neuronal cell death. Biochem Biophys Res Commun. 2003; 304:539–549. [PubMed: 12729589]
37. Millatt LJ, Whitley GS, Li D, Leiper JM, Siragy HM, Carey RM, Johns RA. Evidence for dysregulation of dimethylarginine dimethylaminohydrolase I in chronic hypoxia-induced pulmonary hypertension. Circulation. 2003; 108:1493–1498. [PubMed: 12952847]
38. Miyazaki H, Matsuoka H, Cooke JP, Usui M, Ueda S, Okuda S, Imaizumi T. Endogenous nitric oxide synthase inhibitor: a novel marker of atherosclerosis. Circulation. 1999; 99:1141–1146. [PubMed: 10069780]
39. Moreira PI, Santos MS, Moreno AM, Proenca T, Seica R, Oliveira CR. Effect of streptozotocin-induced diabetes on rat brain mitochondria. J Neuroendocrinol. 2004; 16:32–38. [PubMed: 14962073]
40. Murray AJ, Anderson RE, Watson GC, Radda GK, Clarke K. Uncoupling proteins in human heart. Lancet. 2004; 364:1786–1788. [PubMed: 15541452]
41. Nishio Y, Kanazawa A, Nagai Y, Inagaki H, Kashiwagi A. Regulation and role of the mitochondrial transcription factor in the diabetic rat heart. Ann N Y Acad Sci. 2004; 1011:78–85. [PubMed: 15126286]
42. Papapetropoulos A, Zhou Z, Gerassimou C, Yetik G, Venema RC, Roussos C, Sessa WC, Catravas JD. Interaction between the 90-kDa heat shock protein and soluble guanylyl cyclase: physiological significance and mapping of the domains mediating binding. Mol Pharmacol. 2005; 68:1133–1141. [PubMed: 16024662]
43. Pearce LL, Kanai AJ, Epperly MW, Peterson J. Nitrosative stress results in irreversible inhibition of purified mitochondrial complexes I and III without modification of cofactors. Nitric Oxide. 2005; 13:254–263. [PubMed: 16185902]
44. Petersen KF, Dufour S, Befroy D, Garcia R, Shulman GI. Impaired mitochondrial activity in the insulin-resistant offspring of patients with type 2 diabetes. N Engl J Med. 2004; 350:664–671. [PubMed: 14960743]
45. Porter RK. Mitochondrial proton leak: a role for uncoupling proteins 2 and 3? Biochim Biophys Acta. 2001; 1504:120–127. [PubMed: 11239489]

46. Pritchard K, Stepp D, Konduri G. Inhibition of heatshock protein 90 activity impairs vasorelaxation by increasing superoxide anion generation by endothelial nitric oxide synthase (eNOS). Circulation. 2001 Abstract:500.
47. Pritchard KA Jr, Ackerman AW, Gross ER, Stepp DW, Shi Y, Fontana JT, Baker JE, Sessa WC. Heat shock protein 90 mediates the balance of nitric oxide and superoxide anion from endothelial nitric-oxide synthase. J Biol Chem. 2001; 276:17621–17624. [PubMed: 11278264]
48. Rodriguez AM, Palou A. Uncoupling proteins: gender dependence and their relation to body weight control. Int J Obes Relat Metab Disord. 2004; 28:500–502. [PubMed: 14758347]
49. Ronson RS, Nakamura M, Vinten-Johansen J. The cardiovascular effects and implications of peroxynitrite. Cardiovasc Res. 1999; 44:47–59. [PubMed: 10615389]
50. Sakai K, Matsumoto K, Nishikawa T, Suefuji M, Nakamaru K, Hirashima Y, Kawashima J, Shirotani T, Ichinose K, Brownlee M, Araki E. Mitochondrial reactive oxygen species reduce insulin secretion by pancreatic beta-cells. Biochem Biophys Res Commun. 2003; 300:216–222. [PubMed: 12480546]
51. Salerno JC, Harris DE, Irizarry K, Patel B, Morales AJ, Smith SM, Martasek P, Roman LJ, Masters BS, Jones CL, Weissman BA, Lane P, Liu Q, Gross SS. An autoinhibitory control element defines calcium-regulated isoforms of nitric oxide synthase. J Biol Chem. 1997; 272:29769–29777. [PubMed: 9368047]
52. Schrauwen P, Walder K, Ravussin E. Human uncoupling proteins and obesity. Obes Res. 1999; 7:97–105. [PubMed: 10023736]
53. Schulte TW, Akinaga S, Murakata T, Agatsuma T, Sugimoto S, Nakano H, Lee YS, Simen BB, Argon Y, Felts S, Toft DO, Neckers LM, Sharma SV. Interaction of radicicol with members of the heat shock protein 90 family of molecular chaperones. Mol Endocrinol. 1999; 13:1435–1448. [PubMed: 10478836]
54. Schulte TW, Akinaga S, Soga S, Sullivan W, Stensgard B, Toft D, Neckers LM. Antibiotic radicicol binds to the N-terminal domain of Hsp90 and shares important biologic activities with geldanamycin. Cell Stress Chaperones. 1998; 3:100–108. [PubMed: 9672245]
55. Shah V, Wiest R, Garcia-Cardena G, Cadelina G, Groszmann RJ, Sessa WC. Hsp90 regulation of endothelial nitric oxide synthase contributes to vascular control in portal hypertension. Am J Physiol. 1999; 277:G463–G468. [PubMed: 10444461]
56. Sims NR, Anderson MF. Mitochondrial contributions to tissue damage in stroke. Neurochem Int. 2002; 40:511–526. [PubMed: 11850108]
57. Sullivan PG, Springer JE, Hall ED, Scheff SW. Mitochondrial uncoupling as a therapeutic target following neuronal injury. J Bioenerg Biomembr. 2004; 36:353–356. [PubMed: 15377871]
58. Swick L, Kapatos G. A yeast 2-hybrid analysis of human GTP cyclohydrolase I protein interactions. J Neurochem. 2006; 97:1447–1455. [PubMed: 16696853]
59. Tran CT, Leiper JM, Vallance P. The DDAH/ADMA/NOS pathway. Atheroscler Suppl. 2003; 4:33–40. [PubMed: 14664901]
60. Tribe RM, Poston L. Oxidative stress and lipids in diabetes: a role in endothelium vasodilator dysfunction? Vasc Med. 1996; 1:195–206. [PubMed: 9546938]
61. Vanhoutte PM, Boulanger CM. Endothelium-dependent responses in hypertension. Hypertens Res. 1995; 18:87–98. [PubMed: 7584924]
62. Venema RC, Venema VJ, Ju H, Harris MB, Snead C, Jilling T, Dimitropoulou C, Maragoudakis ME, Catravas JD. Novel complexes of guanylate cyclase with heat shock protein 90 and nitric oxide synthase. Am J Physiol Heart Circ Physiol. 2003; 285:H669–H678. [PubMed: 12676772]
63. Vincent AM, Brownlee M, Russell JW. Oxidative stress and programmed cell death in diabetic neuropathy. Ann N Y Acad Sci. 2002; 959:368–383. [PubMed: 11976211]
64. Wiseman DA, Wells SM, Hubbard M, Welker JE, Black SM. Alterations in zinc homeostasis underlie endothelial cell death induced by oxidative stress from acute exposure to hydrogen peroxide. Am J Physiol Lung Cell Mol Physiol. 2007; 292:L165–L177. [PubMed: 16936243]
65. Wiseman DA, Wells SM, Wilham J, Hubbard M, Welker JE, Black SM. Endothelial response to stress from exogenous Zn2+ resembles that of NOmediated nitrosative stress, and is protected by MT-1 overexpression. Am J Physiol Cell Physiol. 2006; 291:C555–C568. [PubMed: 16723513]

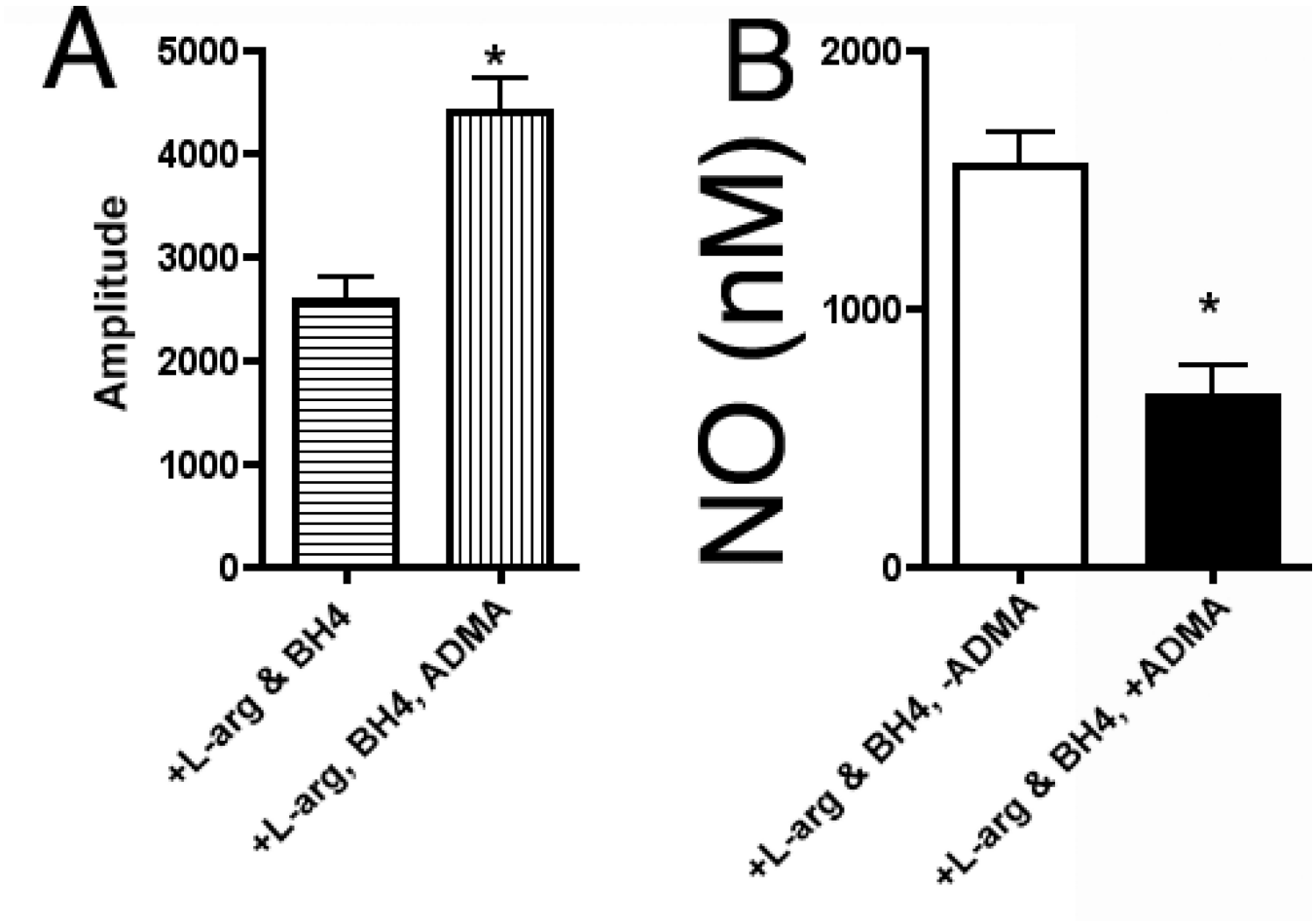

Figure 1.

ADMA uncouples purified recombinant human endothelial NOS. Purified human eNOS (7 pmol) was incubated with 5 μM BH_4, 0.1mM L-arginine, in the presence and absence of 0.1 mM ADMA. ESR was used to determine eNOS superoxide generation over a 20 min incubation period (panel A). Simultaneously NO generation was determined using an NO sensor (Panel B). ADMA significantly increases superoxide generation and decreases NO generation from eNOS. n=6. Values are mean ± SE. * $P<0.05$ vs no ADMA.

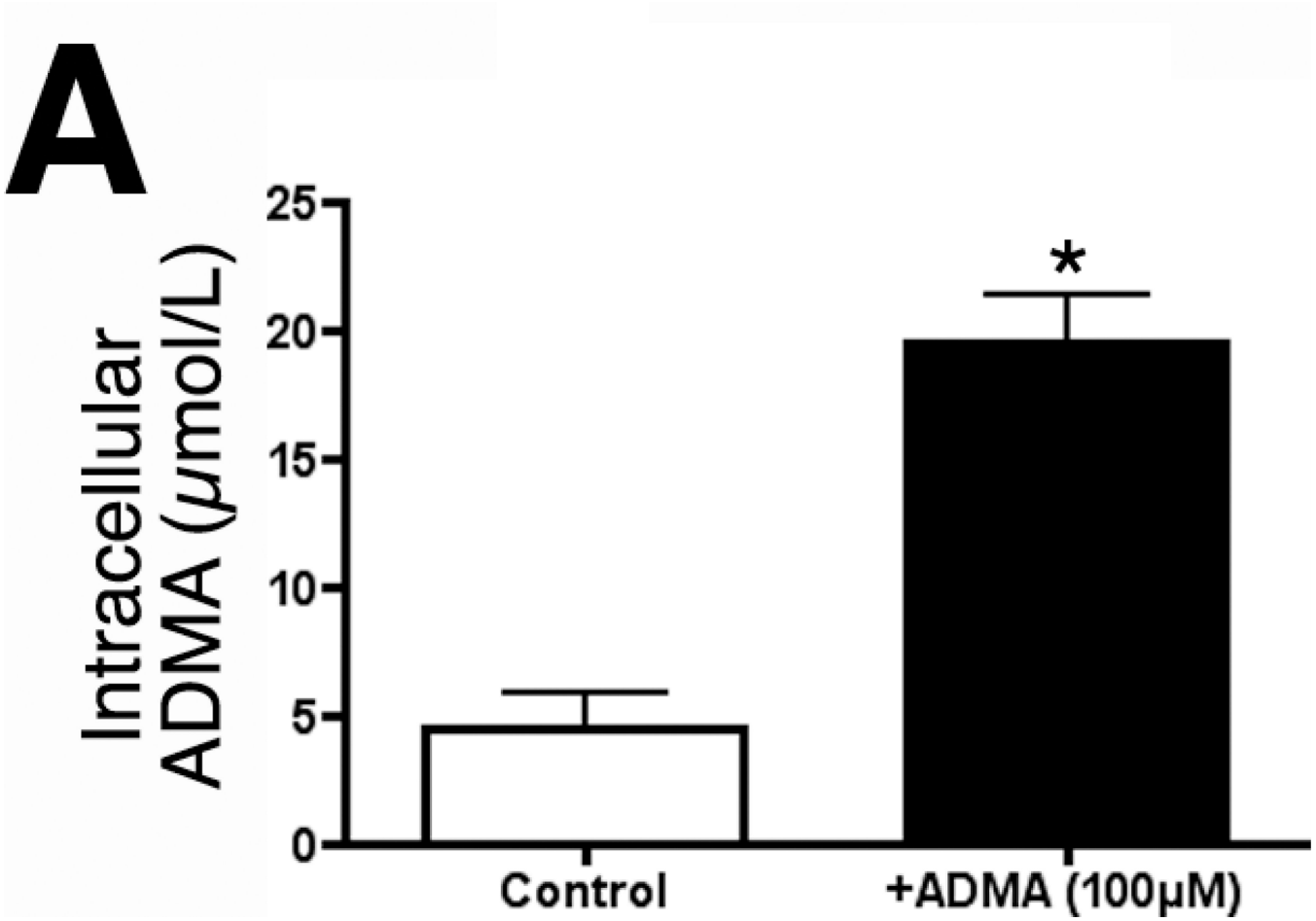

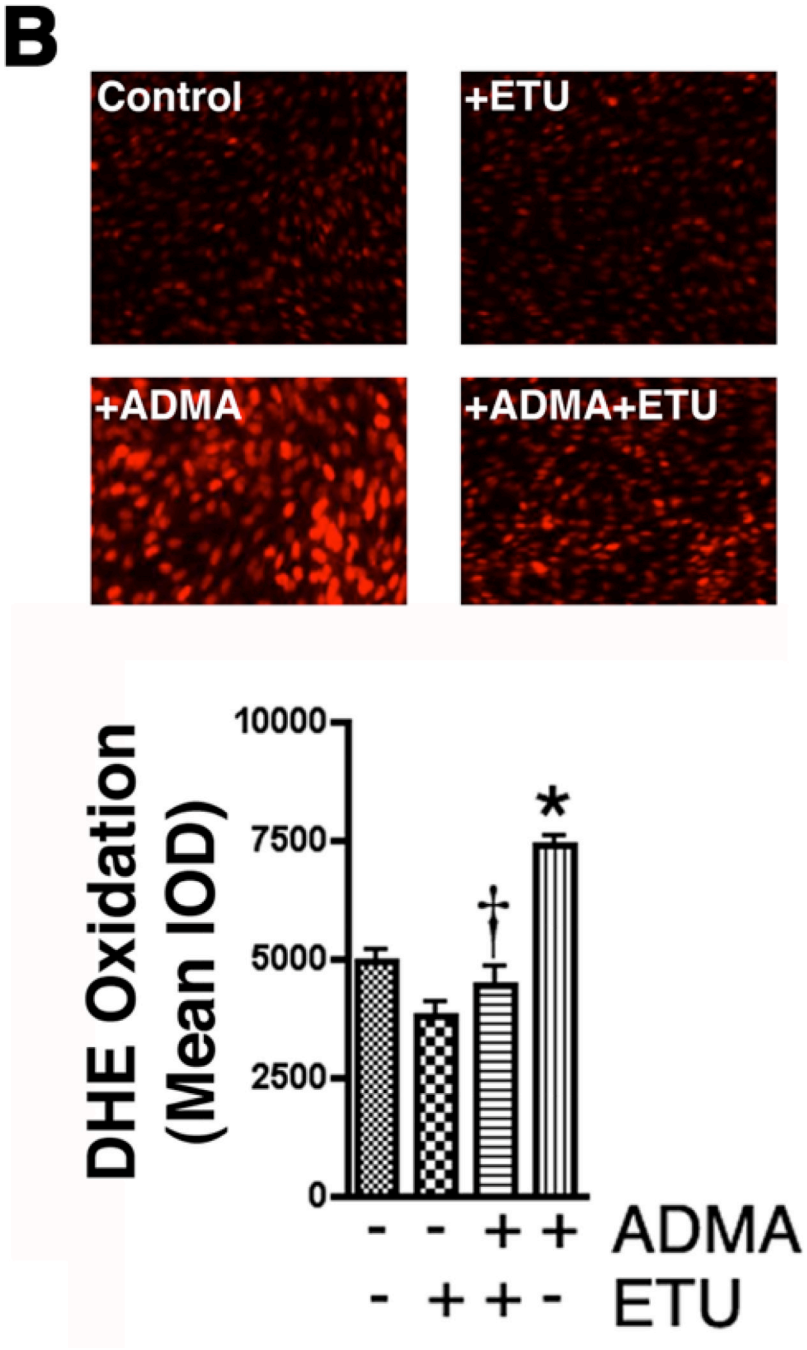

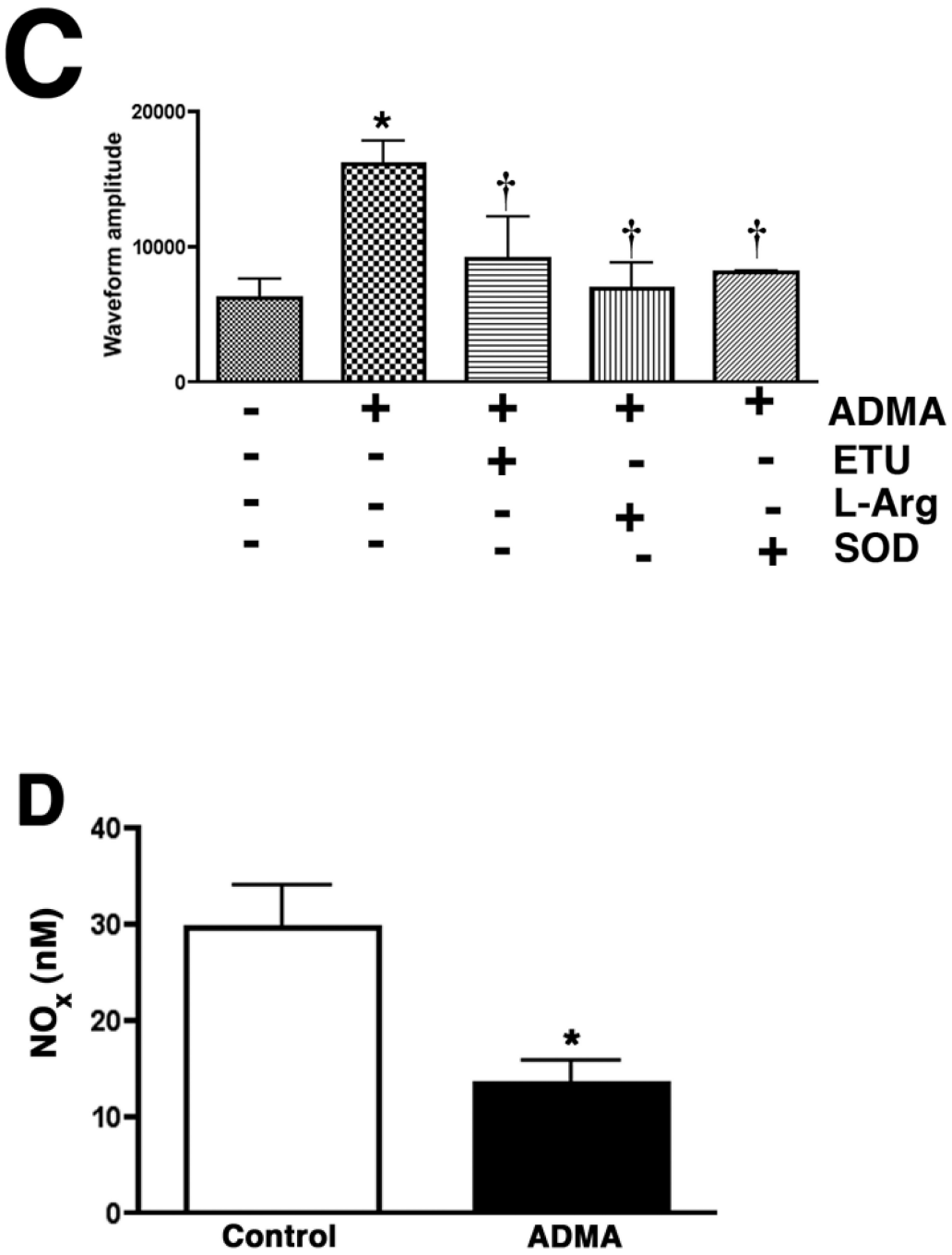

Figure 2.

ADMA induces endothelial NOS uncoupling in pulmonary arterial endothelial cells. PAEC were exposed or not to ADMA (100μM, 1h) then cellular ADMA levels determined (Panel A). In addition, the effect of increased ADMA on cellular superoxide levels were quantified using DHE and fluorescent microscopy (Panel B), or by EPR (Panel C). The effect of ADMA on NO generation was also determined (Panel D). The increased superoxide generation induced by ADMA is blocked by the addition of the NOS inhibitor, ETU (100μM), excess L-arginine (1mM), or PEG-SOD (100 units). NO generation is also decreased, indicating ADMA is uncoupling eNOS. n=4–6. Values are mean ± SE. * $P < 0.05$ vs. Control; † $P < 0.05$ vs. ADMA alone.

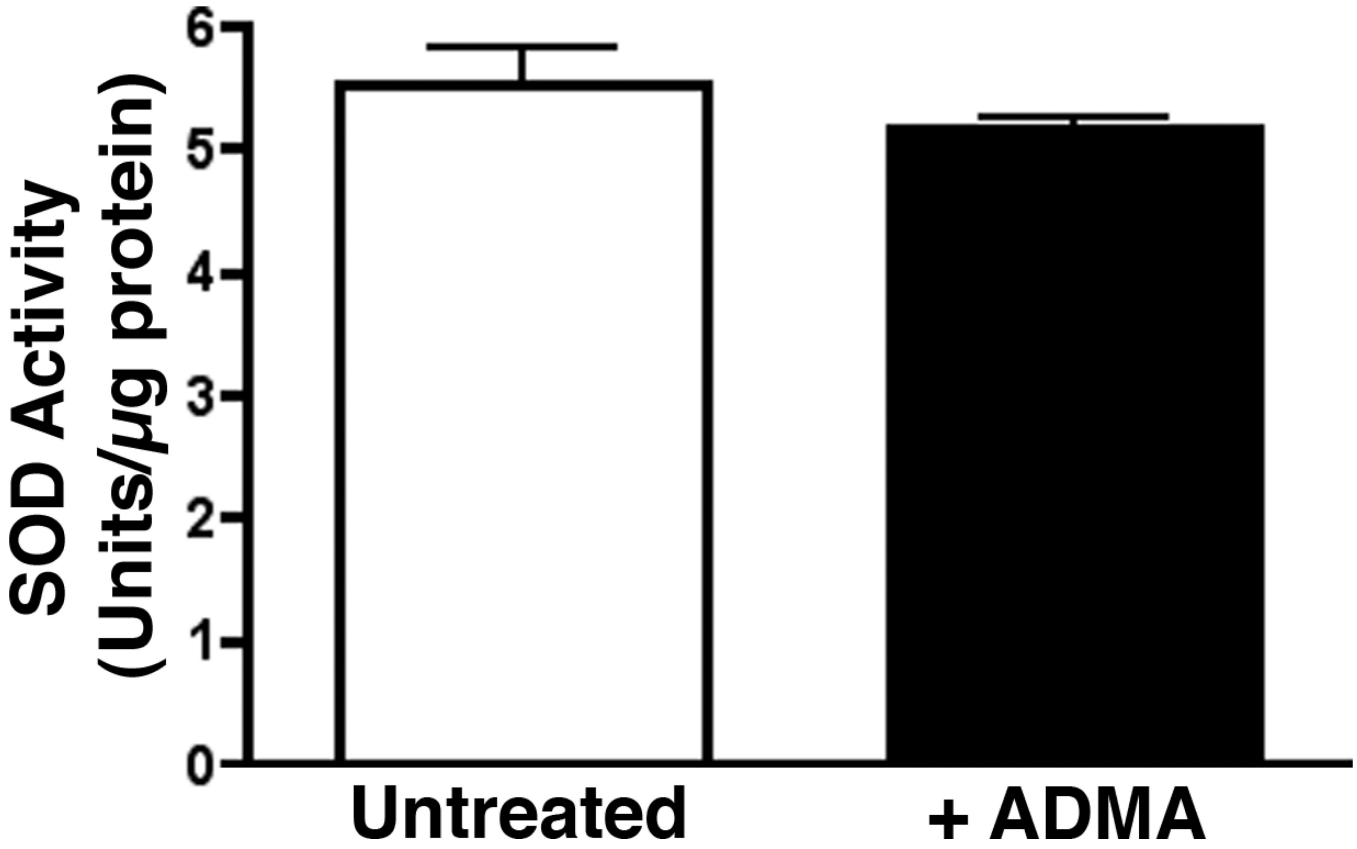

Figure 3.
ADMA does not alter SOD activity in pulmonary arterial endothelial cells. PAEC were exposed or not to ADMA (100μM, 1h) then cellular SOD activity was determined. ADMA exposure does not alter SOD activity. Values are expressed as mean units of activity /μg protein ± SE. N=3.

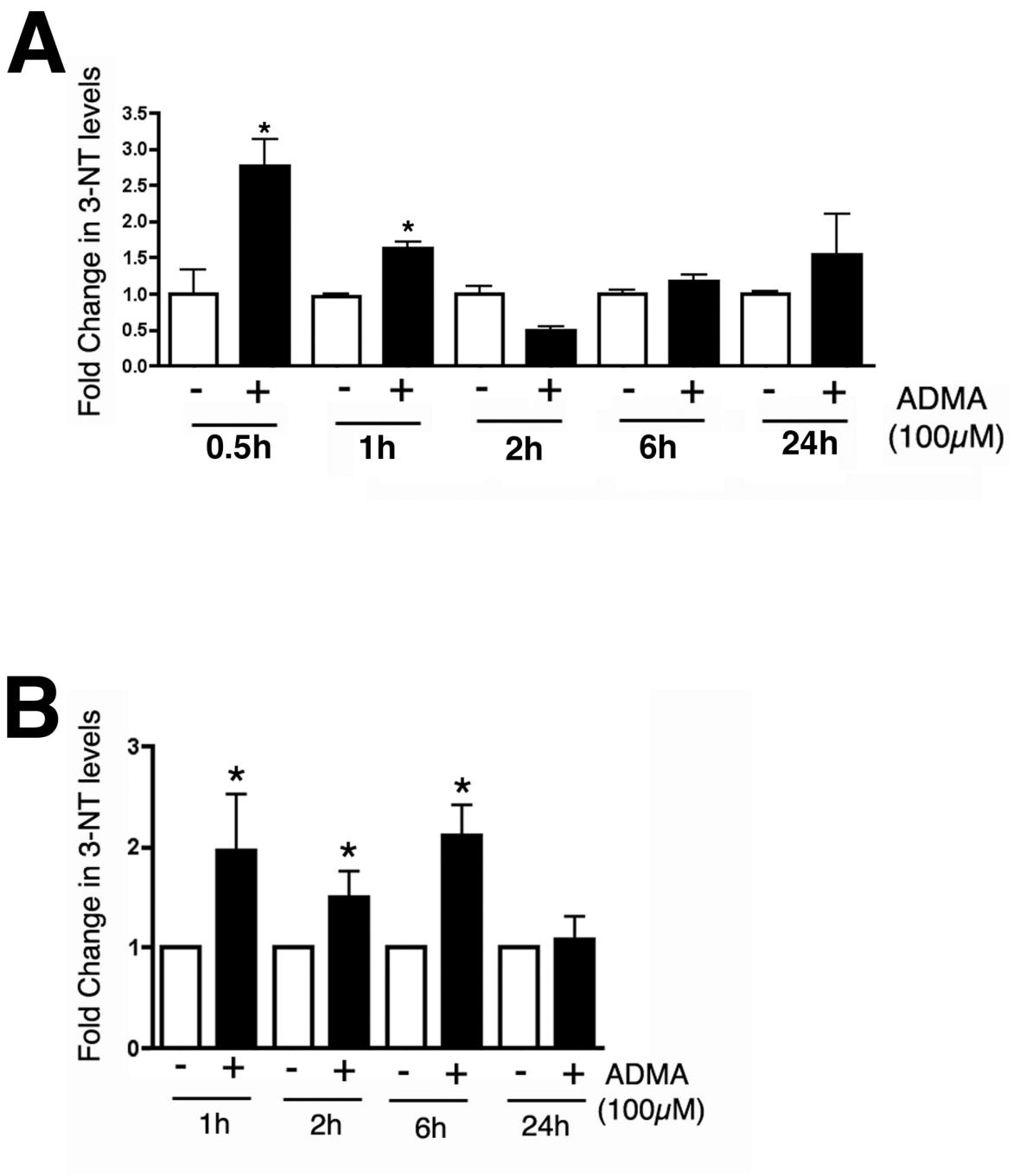

Figure 4.

ADMA exposure increases peroxynitrite levels in pulmonary arterial endothelial cells. Cells were exposed or not to ADMA (100μM) for 0–24h and whole cell extracts (Panel A) or mitochondrial fractions (Panel B) prepared and peroxynitrite exposure estimated using dot-blot analysis to measure 3-NT protein levels. 3-NT levels are increased as early as 0.5h of exposure in the whole cell extracts and are maintained for at least 6h in the mitochondrial fraction. N=6. Values are means ± SE. *P <0.05 vs Control.

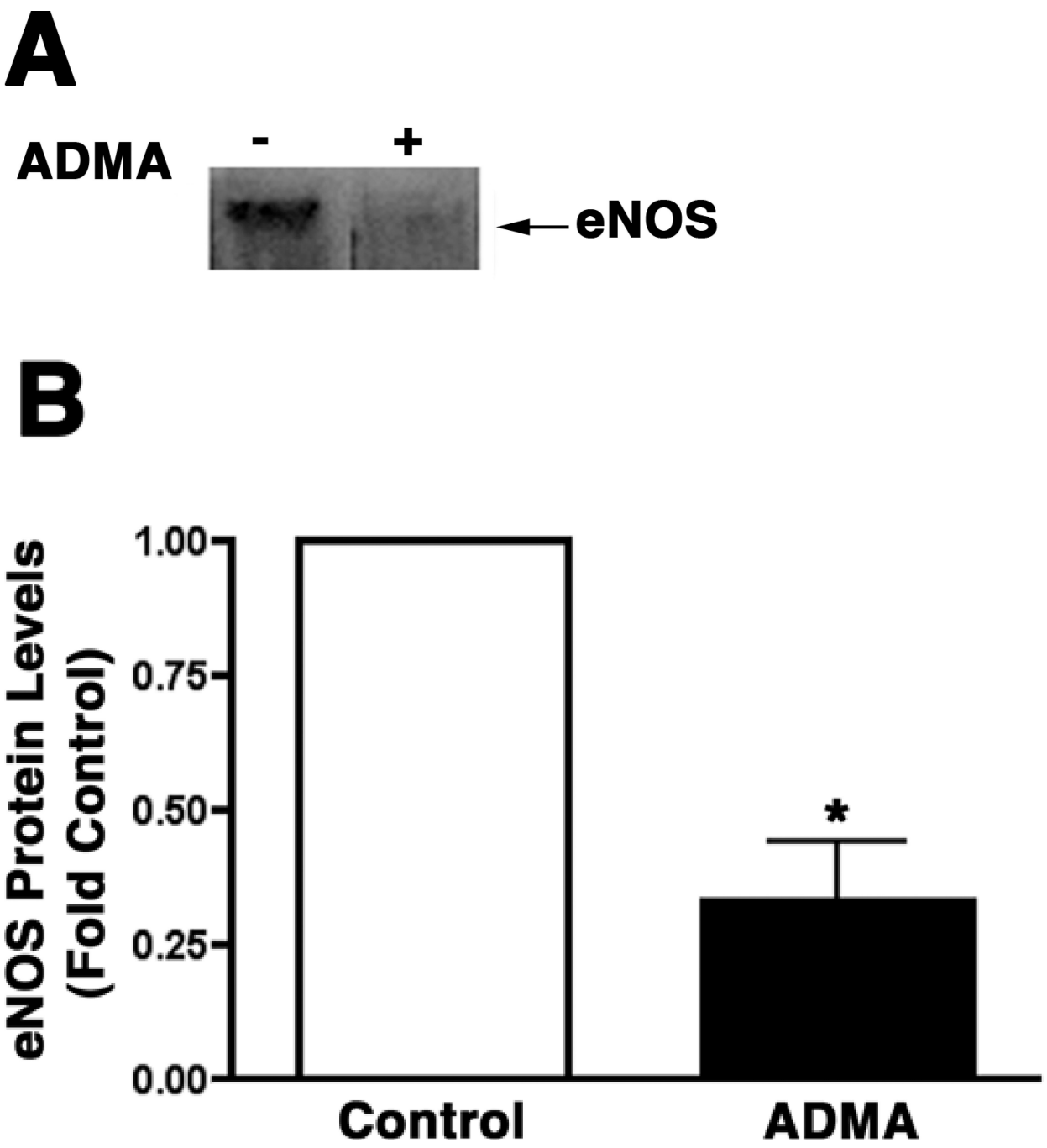

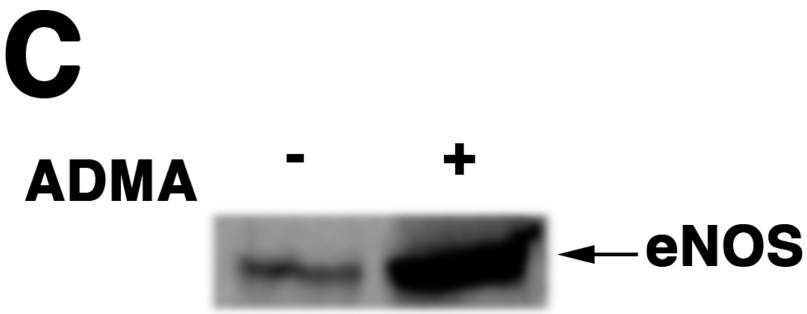

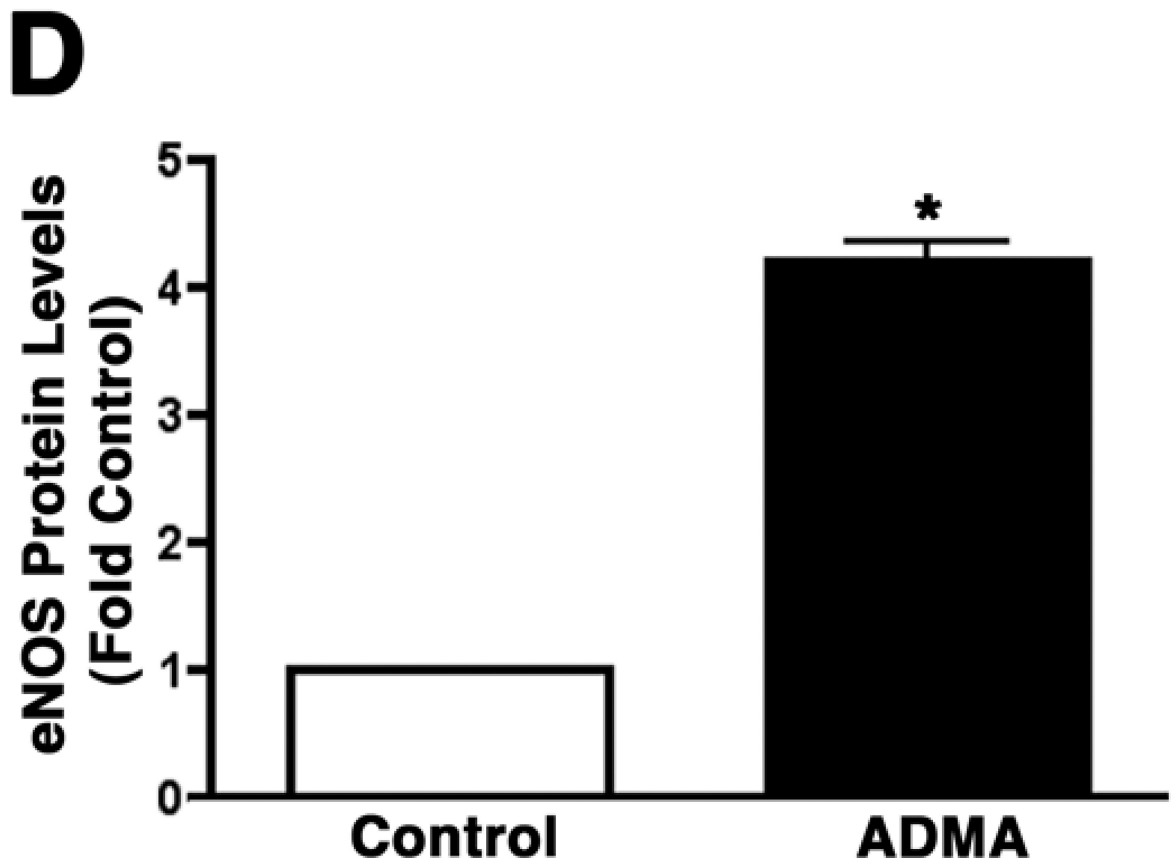

Figure 5.

ADMA induces the redistribution of eNOS in pulmonary arterial endothelial cells. PAEC were treated with ADMA (100μM, 1h). Plasma membrane and mitochondrial fractions were then prepared and protein extracts subjected to Western blot analysis. A representative image is shown for each cell fraction. N=3. Densitometric values are mean ± SE. *P <0.05 vs. Control.

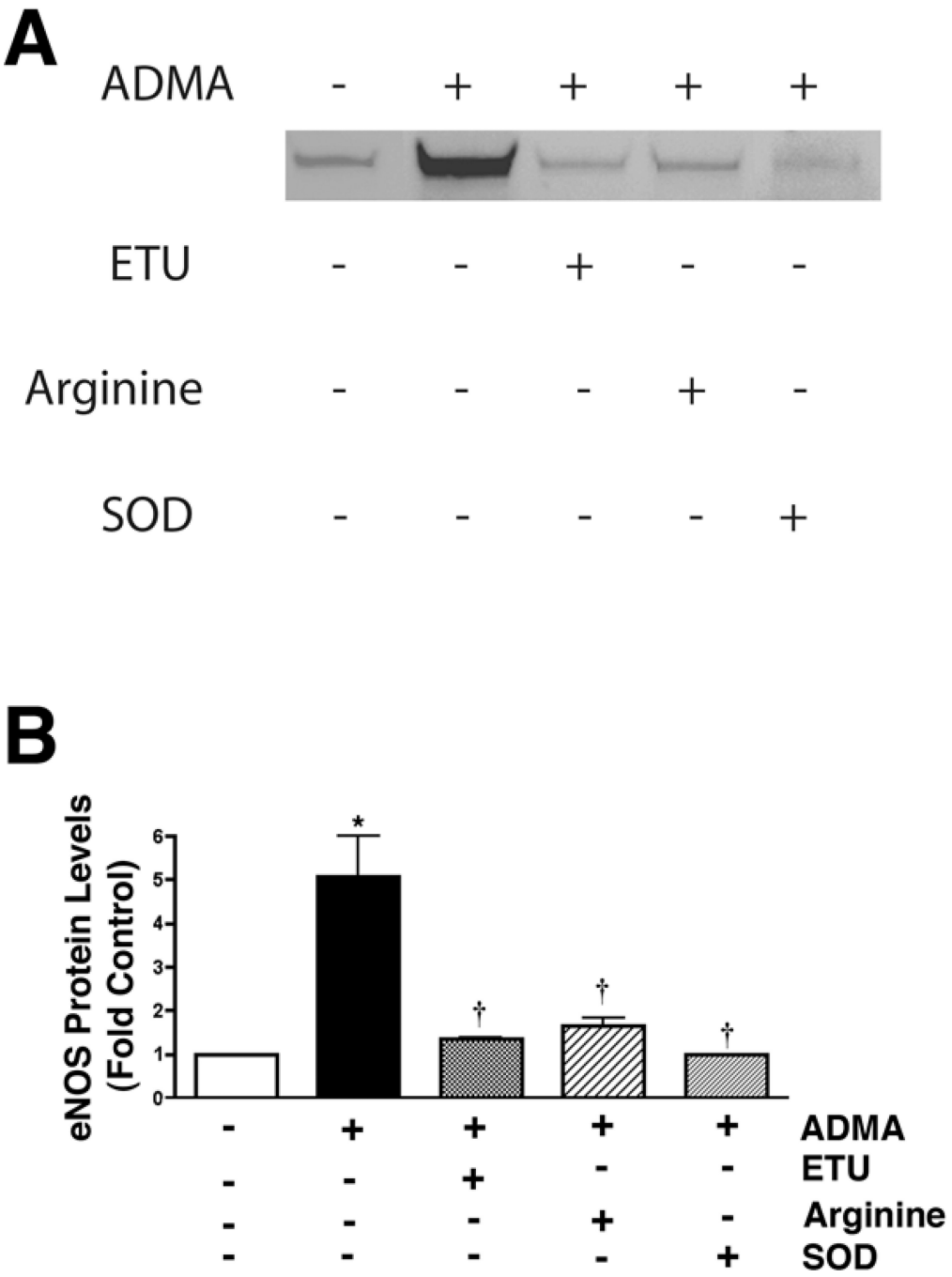

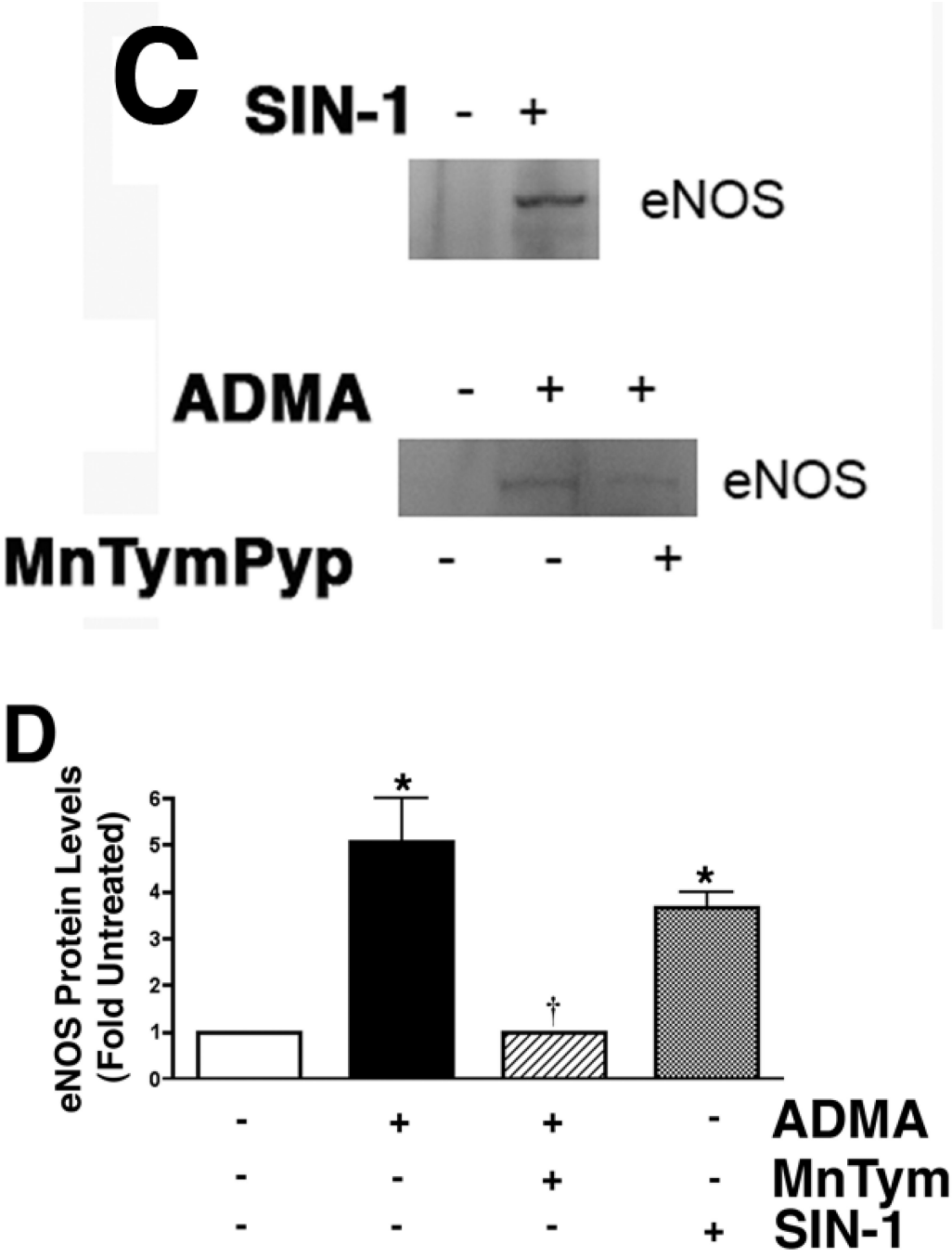

Figure 6.

ADMA-mediated redistribution of eNOS in pulmonary arterial endothelial cells is peroxynitrite dependent. PAEC were treated with ADMA (100μM, 1h) in the presence and absence of the NOS inhibitor, ETU (100μM), L-arginine (1mM), or PEG-SOD (100 units). Mitochondrial fractions were then prepared and protein extracts subjected to Western blot analysis. A representative image is shown (A). Densitomeric values are mean ± SE (B). In addition, cells were treated for 1h with the peroxynitrite generator, SIN-1 (10μM) or ADMA (100μM) with or without the peroxynitrite scavenger MnTymPyp (25μM). A representative image is shown (C). Densitomeric values are mean ± SE (D). N=3. *P <0.05 vs. Control; † P<0.05 vs. ADMA alone.

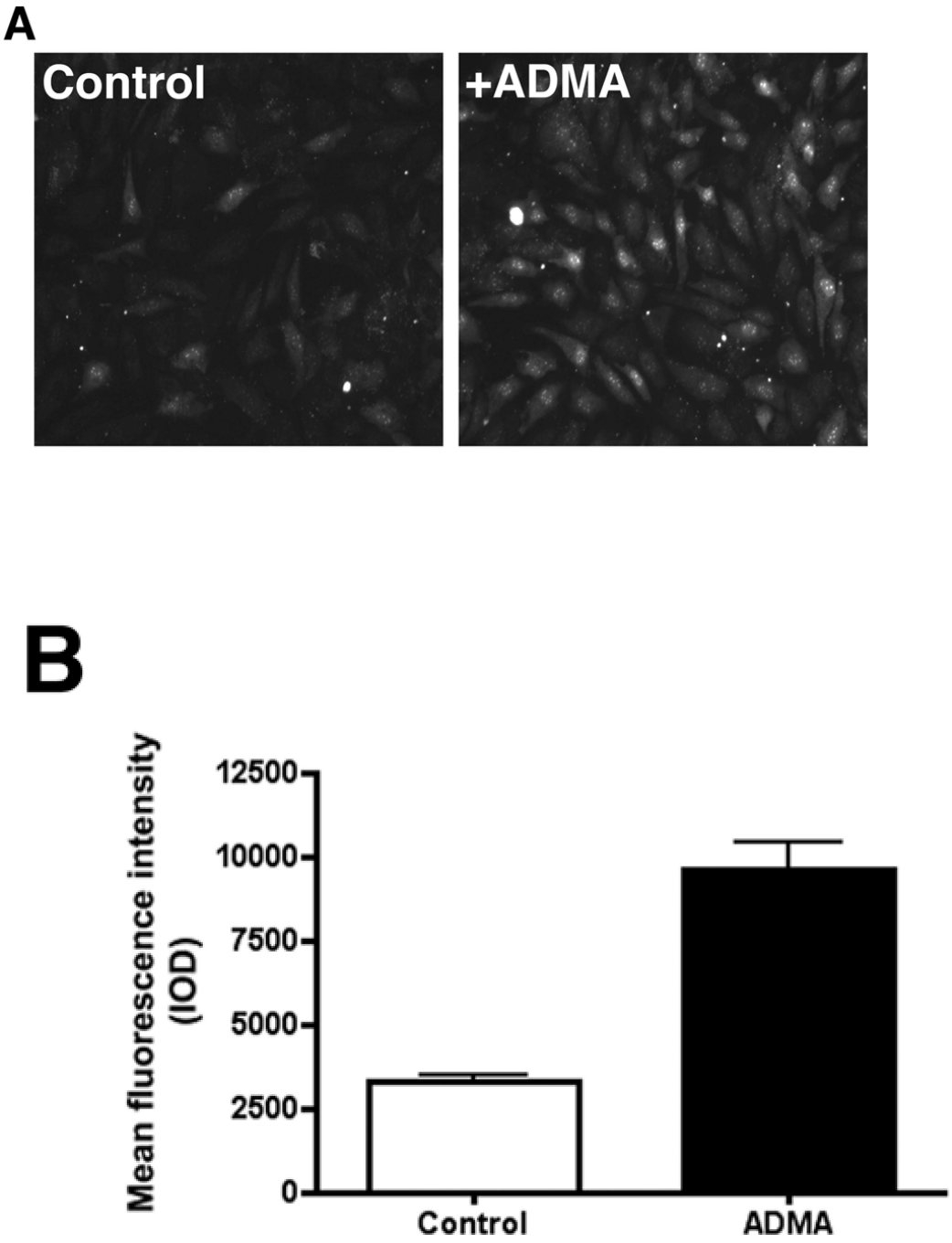

Figure 7.

ADMA induces mitochondrial oxidative stress in pulmonary arterial endothelial cells. Cells were treated with ADMA (100μM, 30 min). MitoSOX red mitochondrial superoxide indicator (Molecular Probes) was added to a final concentration of 5μm and the cells were incubated for another 30 min at 37°C. Cells were washed with PBS and images were captured and the fluorescent intensity of the images (Panel A) was quantified (Panel B). Images of ten random fields were quantified for each sample. n=8. Values are means ± SE. * P<0.05 vs Control.

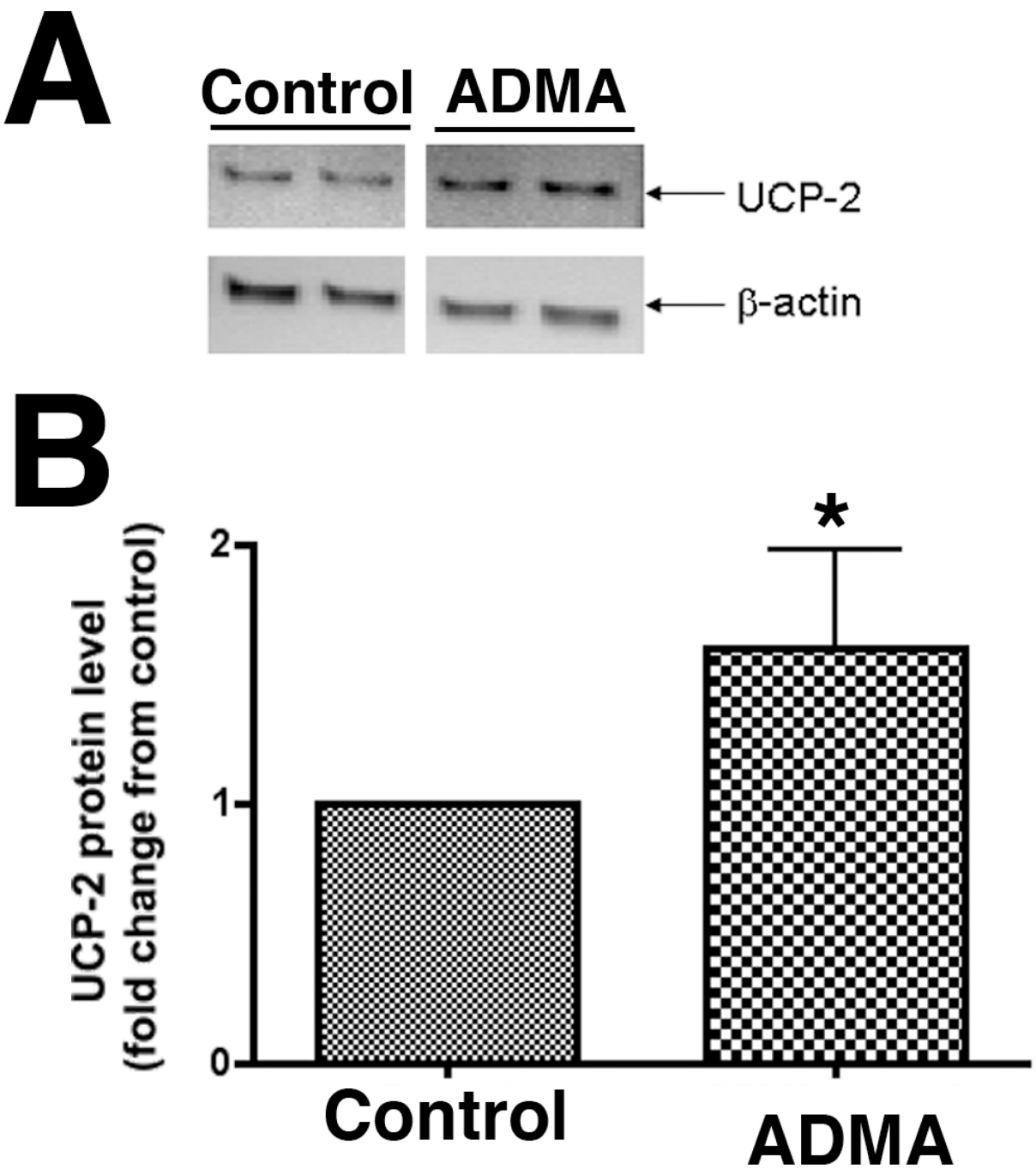

Figure 8.

UCP-2 protein levels are increased in ADMA exposed pulmonary arterial endothelial cells. PAEC treated with ADMA or not (100 μM) for 1h then whole cell protein extracts (10μg) were separated on 4–20% SDS-polyacrylamide gel and electrophoretically transferred to PVDF membranes. The membranes were then subjected to Western blot analysis using a rabbit polyclonal UCP2 antibody. Bands were visualized with chemiluminescence using a Kodak Digital Science Image Station. UCP2 protein levels were then normalized to β-actin protein. A representative blot is shown (Panel A). Densitomeric values were then obtained (Panel B). N=5. Values are mean ± SE. *P <0.05 vs. Control.

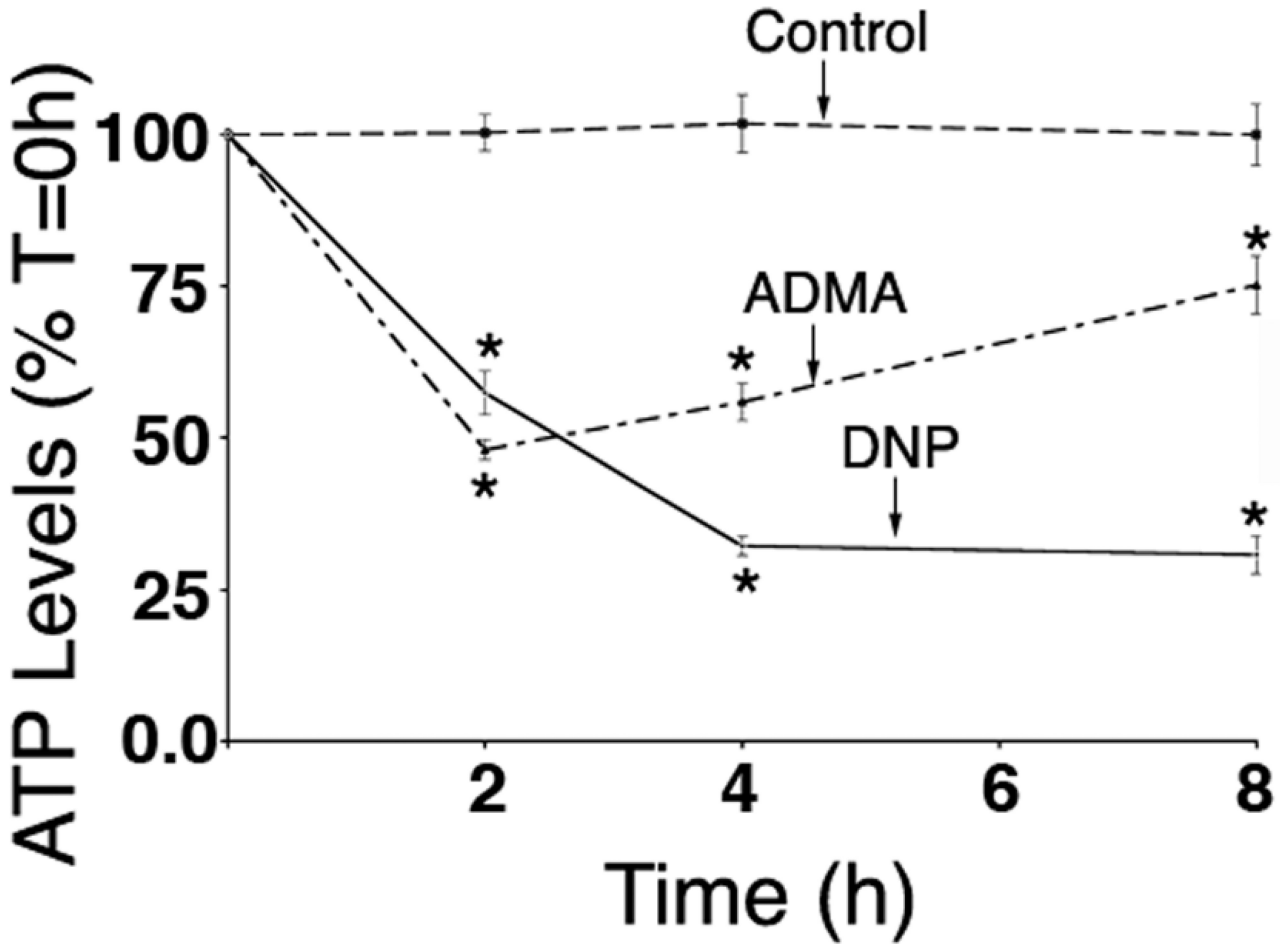

Figure 9.

ADMA exposure decreases cellular ATP levels in pulmonary arterial endothelial cells. Cells were exposed or not to either ADMA (100μM) or the mitochondrial inhibitor 2,4-DNP (50μM, as a positive control for mitochondrial dysfunction) for 0–8h and cellular ATP levels determined using a luciferase-based ATP measurement kit. Both ADMA and 2,4-DNP significantly reduce cellular ADMA levels. N=6. Values are means ± SE. *P <0.05 vs Control.

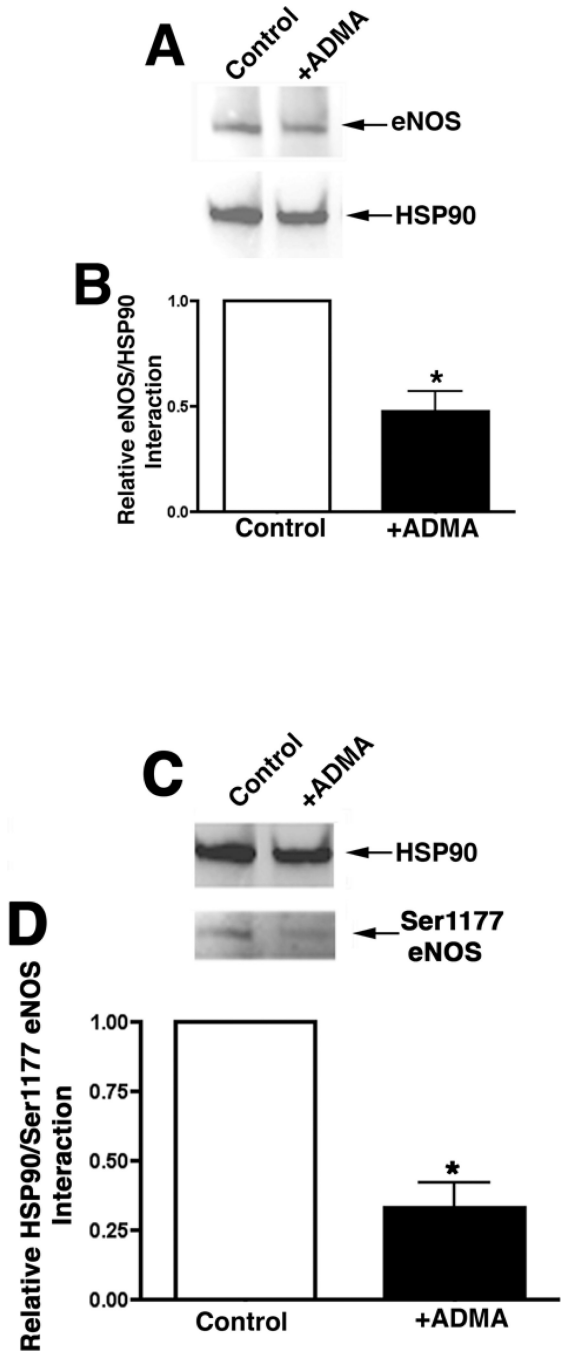

Figure 10.

ADMA disrupts HSP90 activity in pulmonary arterial endothelial cells. PAEC were treated with ADMA (100μM, 1h). Cells were then washed with PBS and lysates prepared with modified RIPA buffer. Immunoprecipitation was performed with using an antibody to HSP90. Protein extracts were separated on 4–20% SDS-polyacrylamide gel and electrophoretically transferred to polyvinylidene difluoride membranes. The membranes were then probed with the appropriate antibodies to either eNOS (Panel A) or S1177 eNOS (Panel C). Representative images are shown. Blots were also stripped and re-probed for HSP90 to normalize for the immunoprecipitation efficiency. Densitomeric values were

obtained for total eNOS (Panel B) and phospho ser1177 eNOS (Panel D) protein. N=5. Values are mean ± SE. *P <0.05 vs. untreated cells.